

^{39}Ar - ^{40}Ar “ages” and origin of excess ^{40}Ar in Martian shergottites

Donald BOGARD^{1*}, Jisun PARK^{1,2}, and Daniel GARRISON^{1,3}

¹ARES, Code KR, NASA Johnson Space Center, Houston, Texas 77058, USA

²Present address: Lunar & Planetary Institute, 3600 Bay Area Blvd., Houston, Texas 77058, USA

³ESCG-Barrios, JE23, 2224 Bay Area Blvd., Houston, Texas 77058, USA

*Corresponding author. E-mail: donald.d.bogard@nasa.gov

(Submitted 15 October 2008; revision accepted 01 April 2009)

Supplementary material is available online at <http://meteoritics.org/Online%20Supplements.htm>

Abstract—We report new ^{39}Ar - ^{40}Ar measurements on 15 plagioclase, pyroxene, and/or whole rock samples of 8 Martian shergottites. All age spectra suggest ages older than the meteorite formation ages, as defined by Sm-Nd and Rb-Sr isochrons. Employing isochron plots, only Los Angeles plagioclase and possibly Northwest Africa (NWA) 3171 plagioclase give ages in agreement with their formation ages. Isochrons for all shergottite samples reveal the presence of trapped Martian ^{40}Ar ($^{40}\text{Ar}_{\text{xs}}$), which exists in variable amounts in different lattice locations. Some $^{40}\text{Ar}_{\text{xs}}$ is uniformly distributed throughout the lattice, resulting in a positive isochron intercept, and other $^{40}\text{Ar}_{\text{xs}}$ occurs in association with K-bearing minerals and increases the isochron slope. These samples demonstrate situations where linear Ar isochrons give false ages that are too old. After subtracting $^{40}\text{Ar}^*$ that would accumulate by ^{40}K decay since meteorite formation and small amounts of terrestrial ^{40}Ar , all young age samples give similar $^{40}\text{Ar}_{\text{xs}}$ concentrations of $\sim 1\text{--}2 \times 10^{-6} \text{ cm}^3/\text{g}$, but a variation in K content by a factor of ~ 80 . Previously reported NASA Johnson Space Center data for Zagami, Shergotty, Yamato (Y-) 000097, Y-793605, and Queen Alexandra Range (QUE) 94201 shergottites show similar concentrations of $^{40}\text{Ar}_{\text{xs}}$ to the new meteorite data reported here. Similar $^{40}\text{Ar}_{\text{xs}}$ in different minerals and meteorites cannot be explained as arising from Martian atmosphere carried in strongly shocked phases such as melt veins. We invoke the explanation given by Bogard and Park (2008) for Zagami, that this $^{40}\text{Ar}_{\text{xs}}$ in shergottites was acquired from the magma. Similarity in $^{40}\text{Ar}_{\text{xs}}$ among shergottites may reveal common magma sources and/or similar magma generation and emplacement processes.

INTRODUCTION

Martian shergottites commonly are classed into three types based on mineralogy: basaltic, lherzolitic (or olivine-, pyroxene-phyric), and olivine-phyric (Goodrich 2002). Basalts are pyroxene-plagioclase rocks that crystallized from fractionated magmas. Lherzolitic shergottites are olivine-pyroxene cumulates, containing much less plagioclase, which also derived from basaltic magmas. The olivine-phyric shergottites consist of a groundmass of pyroxene and plagioclase similar to basaltic shergottites, but contain megacrysts of olivine similar to lherzolites. The crystallization histories of shergottites were not simple. Textures of olivine xenoliths in olivine-phyric shergottites suggest they formed earlier and were assimilated into the groundmass (McSween 1985; Goodrich 2002). Some basaltic shergottites contain cumulus pyroxene indicating an evolving crystallization history as magma rose toward the surface

(McCoy et al. 1992, 1999; McSween et al. 2001). Compositional differences among shergottites have been attributed both to variable assimilation of Martian crust and heterogeneous source regions (Symes et al. 2008 and references therein). One might expect that more differentiated basaltic shergottites would be enriched in incompatible elements such as light REE, and in associated isotopics, in comparison to mafic shergottites. However, no good correlation is observed (Symes et al. 2008).

The formation ages of many shergottites have been determined from the Sm-Nd, Rb-Sr and U-Pb radiometric systems (Borg et al. 2001, 2003, 2005; Nyquist et al. 2001a; Shih et al. 2003, 2005, 2007; Bouvier et al. 2005; Misawa et al. 2006a, 2008). Most dated basaltic shergottites and a few lherzolitic shergottites give formation ages of approximately 170–190 Ma. These shergottites likely derived from a common mantle source through variable amounts of fractional crystallization (Symes et al. 2008; Mikouchi et al.

2008). One dated olivine-phyric shergottite, Northwest Africa (NWA) 1068, gives an age, 182 ± 11 Ma, similar to ages of several basaltic shergottites, whereas, other dated olivine-phyric shergottites give older ages of ~ 445 – 575 Ma (Borg et al. 2001; Borg et al. 2003; Shih et al. 2005; Shih et al. 2007; Symes et al. 2008). Also, one dated basalt, Queen Alexandra Range (QUE) 94201, has a formation age, 327 ± 10 Ma, much older than other basalts (Borg et al. 1997). Interestingly, QUE 94201 derived from a highly differentiated magma, yet is highly depleted in LREE. NWA 1068, on the other hand, with a mafic composition, is relatively LREE enriched.

Those shergottites depleted in incompatible elements are referred to as depleted shergottites, and meteorites enriched in these elements are called enriched shergottites. Warren and Bridges (2005) suggested classifying shergottites based on the degree of enrichment or depletion, and pointed out that the degree of depletion correlates with initial Sr and Nd isotopic ratios. In this type of classification, many basalts are enriched, many olivine-phyric types are depleted, and most lherzolites show intermediate depletion. By one interpretation, the major element composition and radiogenic isotopic systematics of depleted shergottites were primarily controlled by their source regions and fractional crystallization, whereas relatively high proportions of an assimilate are invoked for the enriched shergottites (Warren and Bridges 2005; Symes et al. 2008). It is not clear whether this assimilation involves a common crustal component or is a more complex process (Nyquist et al. 2001b; Warren and Bridges 2005; Symes et al. 2008). Enriched shergottites derived from source regions very similar to each other, but different from source regions of the depleted and intermediate groups, and these sources likely formed early in Martian history (Herd et al. 2002; Symes et al. 2008). Symes et al. (2008) suggested possible relationships among mantle sources of various shergottites. They place enriched (mostly basaltic) shergottites with formation ages around 170 Ma in a common magma chamber, and possibly include olivine-phyric NWA 1068 with this group. These authors suggest that intermediate (lherzolitic) shergottites with ages < 200 Ma derived from a different source. Strongly depleted shergottites with older ages may have derived from a common source region, which was distinct from the above source regions.

Determined ^{39}Ar - ^{40}Ar ages of nearly all shergottites are higher than formation ages determined by other radiometric techniques. In some analyses this is caused by the presence of shock implanted, Martian atmospheric ^{40}Ar (Bogard and Garrison 1999; Walton et al. 2007). However, isochron plots of Ar-Ar data obtained at NASA Johnson Space Center (JSC) on whole rock and mineral separates of many shergottite samples do not suggest the variable presence of shock-implanted Martian atmospheric ^{40}Ar , but rather a ^{40}Ar component more uniformly distributed in the lattice of various minerals. In a recent Ar-Ar study of separated minerals from the Zagami shergottite, Bogard and Park

(2008) argue that the ^{40}Ar in excess of that which would form in the last ~ 170 Ma was acquired from the magma and is not shock-implanted Martian atmospheric ^{40}Ar . In this paper we present Ar-Ar results obtained on several shergottites spanning the above shergottite classifications. All of these shergottites show apparent Ar-Ar ages older than the formation ages determined by other radiometric techniques. Using enhanced isochron techniques, we also identify the excess Martian ^{40}Ar components in each sample and estimate their concentrations. We show that for some shergottites this excess ^{40}Ar is nearly constant across extractions, whereas other excess ^{40}Ar is released in association with ^{39}Ar produced from K. We argue from these data that, like Zagami, several shergottites have inherited trapped ^{40}Ar from the magma, and that this implies similar magma sources or generation processes.

SAMPLES AND METHODS

Brief descriptions of the shergottites we analyzed and of the sources of our samples are given in Appendix 1. Including data previously reported, shergottites analyzed at JSC include basaltic, lherzolitic, and olivine-phyric types, being both trace element enriched and trace element depleted, showing a factor of two range in shock levels, and possessing different degrees of terrestrial weathering. We will refer to whole rock samples as WR and to mineral separates as Plag (plagioclase) and Pyx (pyroxene). Most of our mineral separates were prepared at JSC, primarily by C–Y Shih or Y. Reese. A crushed, $< 297 \mu\text{m}$ size separate of Los Angeles was separated into plagioclase and pyroxene by magnetic susceptibility using a Frantz magnetic separator, and Plag, Pyx and WR were analyzed. A chip was taken from a 13.6 g interior sample of NWA 3171, was crushed, and the 100–200 mesh (149–74 μm) fraction was utilized. Plagioclase was first separated by low magnetic susceptibility, and then was concentrated using heavy liquid with a density cut at $< 2.85 \text{ g/cm}^3$. From a 2.2 g exterior sample, a chip was taken from a dark impact glass vein (NWA 3171 Glass). A plagioclase sample of NWA 2975 was obtained by magnetic susceptibility. At JSC, L. Borg washed an uncrushed piece of Dhofar (Dho) 019 in acetone and acid leached it with sonication. Plagioclase was separated from a 100–200 mesh sieve fraction using a Frantz magnetic separator, followed by hand-picking. A 100–200 mesh fraction of Dar al Gani (DaG) 476 was first separated into minerals using magnetic susceptibility, then plagioclase was further concentrated using heavy liquids with a density cut at $< 2.85 \text{ g/cm}^3$. Two different pyroxenes, labeled ‘Light or LT’ (Mg-rich) and ‘Dark or DK’ (Fe-rich), were obtained with density cuts at $2.96 < \rho < 3.32 \text{ g/cm}^3$ and $3.32 < \rho < 3.45 \text{ g/cm}^3$, respectively. Note that plagioclase in all shergottites has been shocked sufficiently to structurally convert to maskelynite, but retains the plagioclase chemical composition (Fritz et al. 2005).

For the new ^{39}Ar - ^{40}Ar data reported here, samples were irradiated in 8 separate irradiations over the years 1999 to 2006. Multiple samples of hornblende NL-25 (~2–4 mg, or ~1,000 grains each sample) were included in each irradiation as flux and age monitors. Irradiation factors (J-values) for the samples are presented in Table 1. The typical ^{39}Ar production rate for these irradiations was $1.3 \times 10^{-6} \text{ cm}^3/\text{g-K}$ per hour of irradiation. More details of irradiation parameters were discussed in Appendix A of Nyquist et al. (2006). Each sample was heated in increasing temperature steps (typically 20 min each) in a Ta furnace equipped with a thermocouple. Ar released was cleaned on active metal getters, and its isotopic composition was measured on a VG-3600 mass spectrometer. Instrument sensitivity was determined occasionally using a calibrated gas pipette. Isotopic data were corrected for blanks, radioactive decay and reactor interferences. Details about experimental procedures and the NL-25 hornblende are given in Bogard et al. (1995, 2000). Measured Ar data are given in an Electronic Annex.

RESULTS OF ARGON-ARGON ANALYSES

Examining Ar-Ar Data from Shergottites

To evaluate ^{39}Ar - ^{40}Ar data for analyses presented here, we utilize both Ar-Ar age spectra and Ar isochron plots. However, the isochron plots we employ are not the commonly used ones, and some have characteristics with which many readers may not be familiar. Appendix 2 discusses in detail the types of Ar components present in Martian shergottites and our use and interpretation of some non-standard isochron plots. Here we very briefly summarize some of the isochron features that appear in our data presentations below.

Isochron plots are typically normalized to ^{36}Ar . Because of the presence of multiple ^{36}Ar components in Martian shergottites, we prefer to normalize isochrons to ^{37}Ar . We also examined isochrons normalized to cosmogenic ^{36}Ar ($^{36}\text{Ar}_{\text{cos}}$) and trapped ^{36}Ar ($^{36}\text{Ar}_{\text{trap}}$). Techniques to separate total ^{36}Ar into $^{36}\text{Ar}_{\text{cos}}$ and $^{36}\text{Ar}_{\text{trap}}$ are described in Appendix 2. Most ^{36}Ar in these samples is $^{36}\text{Ar}_{\text{cos}}$. As an estimate of the reliability of our calculations of $^{36}\text{Ar}_{\text{cos}}$ in individual samples, we compare our calculated $^{36}\text{Ar}_{\text{cos}}$ with literature data on $^{36}\text{Ar}_{\text{cos}}$. A few isochron plots suggests negative intercepts on the normalized ^{40}Ar axis, and Appendix 2 gives likely explanations for such intercepts. For several of our analyzed samples (particularly hot desert meteorites), terrestrial and/or Martian weathering has affected the Ar data for the first few extractions (Appendix 2), and we typically exclude these data from our evaluations.

Data for most of our sample analyses plot above a hypothetical Ar isochron passing through zero and having a slope equivalent to the formation age of the meteorite, as determined by other chronometers, such as Sm-Nd, and Rb-Sr. Some samples even show a relatively linear isochron

slope, but one whose corresponding age is greater than the formation age. These isochron characteristics and the old apparent ages indicated by Ar-Ar age spectra indicate that virtually all of our shergottite samples contained trapped or excess ^{40}Ar ($^{40}\text{Ar}_{\text{xs}}$) above that ^{40}Ar produced in the sample since its formation ($^{40}\text{Ar}^*$). Thus most isochron “ages” presented here are not real K-Ar ages. For reasons presented by Bogard and Park (2008), we reject the argument that shergottites formed ~4 Ga ago and thus contain radiogenic ^{40}Ar not completely degassed in some later event which also reset their Sm-Nd, Rb-Sr, and Pb-Pb ages (Bouvier et al. 2005, 2008). These younger radiometric ages are interpreted by most workers as true shergottite formation times (Borg et al. 2001, 2003, 2005; Nyquist et al. 2001a; Shih et al. 2003, 2005, 2007; Misawa et al. 2006a, 2008). The main result of this work is not to report the true Ar-Ar age, which generally is not possible from these data, but rather to characterize the total concentration of excess Martian ^{40}Ar in each sample that is not produced by in situ decay. We do this in the following sub-sections. Then, we show that these excess ^{40}Ar concentrations are similar among many shergottites, and we argue that this implies interesting consequences for shergottite genesis.

Los Angeles

The Ar-Ar age spectra for WR and Plag samples of Los Angeles are shown in Fig. 1. The reported formation age for Los Angeles is $170 \pm 8 \text{ Ma}$ (Nyquist et al. 2001a). The Plag Ar-Ar age increases slowly with extraction temperature from ~0.20 Ga to ~0.26 Ga, and the K/Ca ratio decreases modestly from ~0.1 to ~0.04. Much higher ages and $^{36}\text{Ar}/^{37}\text{Ar}$ ratios for the first two Plag extractions (0–0.04% ^{39}Ar release) indicate release of adsorbed terrestrial atmospheric Ar, and we do not further consider these data. The $^{36}\text{Ar}/^{37}\text{Ar}$ ratios for the remaining Plag extractions are nearly constant and suggest that the much of the total ^{36}Ar released ($3.5 \times 10^{-9} \text{ cm}^3/\text{g}$) was cosmogenic. If we assume that all ^{36}Ar is cosmogenic in the minimum measured $^{36}\text{Ar}/^{37}\text{Ar}$ ratio and use the other $^{36}\text{Ar}/^{37}\text{Ar}$ ratios to calculate the proportion of $^{36}\text{Ar}_{\text{cos}}$ (Garrison et al. 2000), we obtain a total $^{36}\text{Ar}_{\text{cos}}$ value of $2.8 \times 10^{-9} \text{ cm}^3/\text{g}$. This value is similar to $^{36}\text{Ar}_{\text{cos}} = 2.5\text{--}3.2 \times 10^{-9} \text{ cm}^3/\text{g}$ reported in the literature for unirradiated Los Angeles whole rock (Garrison and Bogard 2000; Eugster et al. 2002; Park 2005). At most a relatively small amount of trapped Martian ^{36}Ar could have been released throughout the Plag extraction. The Los Angeles WR ages are much more variable and range over ~0.16–0.75 Ga. The WR K/Ca decreases from ~0.2 to ~0.01 at high temperatures, where Ar was mostly released from pyroxene. The WR also released more total ^{36}Ar , $4.85 \times 10^{-9} \text{ cm}^3/\text{g}$. Using the minimum $^{36}\text{Ar}/^{37}\text{Ar}$ to calculate $^{36}\text{Ar}_{\text{cos}}$ for the WR gives a value of $3.4 \times 10^{-9} \text{ cm}^3/\text{g}$, suggesting release of a greater amount of trapped ^{36}Ar compared to the Plag.

Table 1. Isochron “ages” (Ma), isochron intercept ratios, and J-values for analyzed samples.

| Meteorite/phase | Isochron data when normalized to: | | | | J-values |
|--------------------|--|------------------------|----------------------|-----------------------|-------------------|
| | ^{37}Ar | Total ^{36}Ar | Cos ^{36}Ar | Trap ^{36}Ar | |
| Los Angeles | | | | | |
| Plag age (Ma) | 165 ± 7 | 148 ± 53 | 170 ± 14 | | 0.02097 ± 0.00008 |
| Plag intercept | 0.193 ± 0.019 | 330 ± 201 | 302 ± 77 | | |
| WR age (Ma) | 318 ± 3 | | 291 ± 12 | 0.02200 ± 0.00004 | |
| WR intercept | 0.166 ± 0.003 | | | 187 ± 10 | |
| NWA 3171 | | | | | |
| Plag age (Ma) | 232 ± 7 | 229 ± 28 | | | 0.02090 ± 0.00008 |
| Plag intercept | 0.057 ± 0.017 | 100 ± 99 | | | |
| NWA 2975 | | | | | |
| Plag age (Ma) | 672 ± 8 | | | 366 ± 3 | 0.02310 ± 0.0010 |
| Plag intercept | -0.173 ± 0.008 | | | 816 ± 19 | |
| Dho 019 | | | | | |
| Plag age (Ma) | 721 ± 41 | 710 ± 72 | | 707 ± 16 | 0.02063 ± 0.00008 |
| Plag intercept | -0.047 ± 0.031 | -14 ± 19 | | 165 ± 43 | |
| WR age (Ma) | 849 ± 25 | | | | 0.02063 ± 0.00008 |
| WR intercept | -0.028 ± 0.009 | | | | |
| DaG 476 | | | | | |
| Plag | Total age = 1.0 Ga, 4–100% ^{39}Ar | | | | 0.02311 ± 0.0011 |
| WR | Total age = 1.40 Ga, 7–100% ^{39}Ar | | | | 0.03118 ± 0.00008 |
| Pyx-light | Total age = 0.85 Ga, 0–100% ^{39}Ar | | | | 0.02215 ± 0.0010 |
| Pyx-dark | Total age = 2.9 Ga, 7–100% ^{39}Ar | | | | 0.02210 ± 0.0010 |
| NWA 1068 WR | | | | | |
| | Total age = 0.34 Ga, 2–100% ^{39}Ar | | | | 0.02555 ± 0.00025 |
| Y-980459 WR | | | | | |
| | Total age = 1.0 Ga, 0–100% ^{39}Ar | | | | 0.02635 ± 0.00013 |
| SaU 005 WR | | | | | |
| | Total age = 2.2 Ga, 0–100% ^{39}Ar | | | | 0.02560 ± 0.00020 |

Isochron-derived “ages” are given with four possible normalizing isotopes: ^{37}Ar , total ^{36}Ar , cosmogenic ^{36}Ar , and trapped ^{36}Ar . Only isochron ages for Los Angeles Plag and possibly NWA Plag approximate formation ages, and all other isochron “ages” have been increased by the presence of trapped Martian ^{40}Ar . Ages listed for DaG 476, NWA 1068, Y-980459, and SaU 005 are total apparent ages averaged over the ranges indicated, and isochron ages for these samples are not defined. All uncertainties are one-sigma.

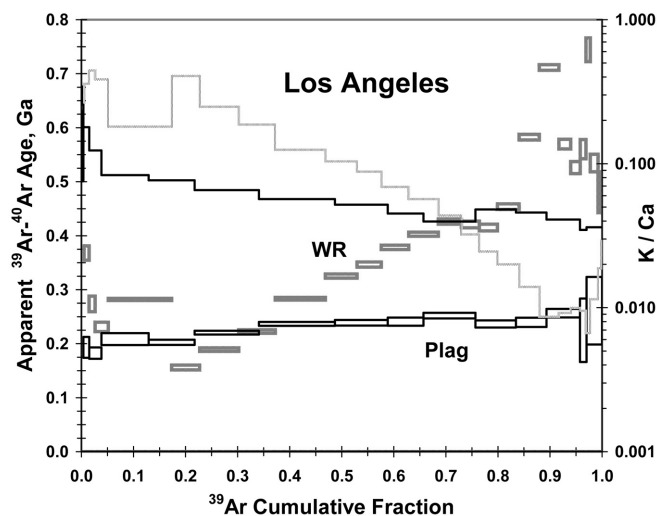


Fig. 1. ^{39}Ar - ^{40}Ar age spectra (rectangles, left Y-axis) and K/Ca ratios (stepped lines, right Y-axis) as a function of cumulative ^{39}Ar release for whole rock (fuzzy lines) and plagioclase (sharp lines) samples of Los Angeles. Age uncertainties ($\sim 1\sigma$) are indicated by the width of the rectangles. Formation ages for Los Angeles and other shergottites studied here are given in Table 2.

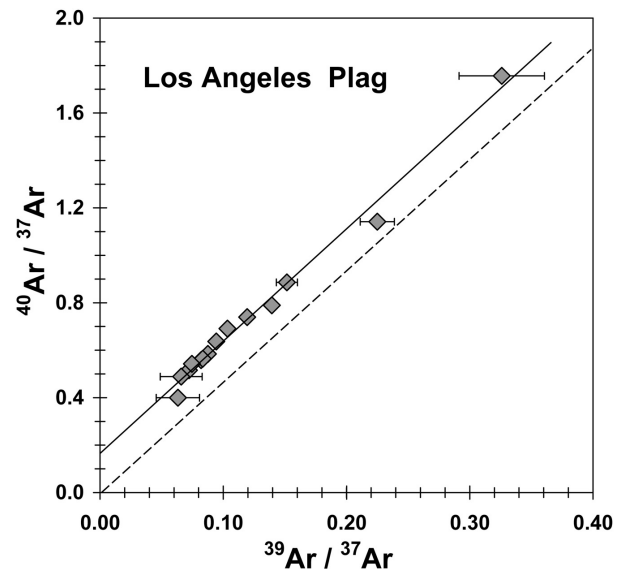


Fig. 2. Plot of $^{40}\text{Ar}/^{37}\text{Ar}$ versus $^{39}\text{Ar}/^{37}\text{Ar}$ for 0.04–100% ^{39}Ar release of Los Angeles Plag. Individual ratio uncertainties are indicated or are smaller than plotted symbols. The solid line is the best fit to the data. The dashed line is a hypothetical isochron through the origin and representing a formation age of 170 Ma.

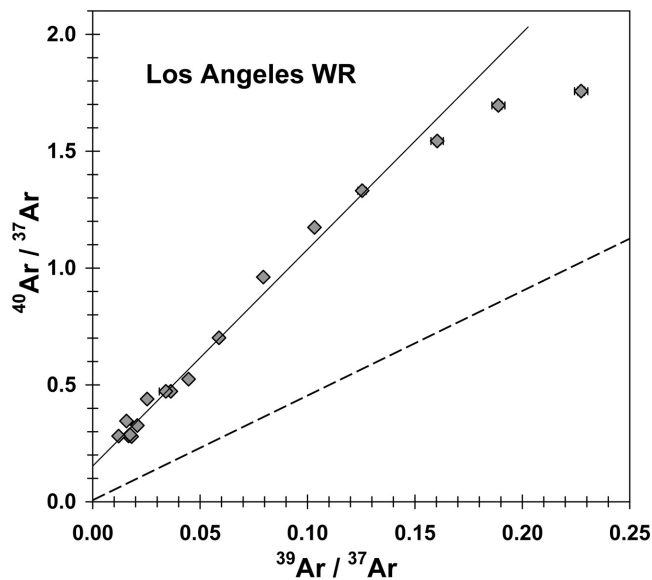


Fig. 3. Plot of $^{40}\text{Ar}/^{37}\text{Ar}$ versus $^{39}\text{Ar}/^{37}\text{Ar}$ for extractions releasing 37–100% of the ^{39}Ar for Los Angeles WR. Individual ratio uncertainties are indicated or are smaller than plotted symbols. The solid line, fitted to only the 57–100% ^{39}Ar data, would represent an age of 343 Ma. A hypothetical isochron through the origin and representing a formation age of 170 Ma is shown by the dashed line.

Figure 2 is an isochron plot of $^{40}\text{Ar}/^{37}\text{Ar}$ versus $^{39}\text{Ar}/^{37}\text{Ar}$ for extractions releasing 0.04–100% of the ^{39}Ar from Los Angeles Plag. The isochron shown gives an age of 165 ± 7 Ma. If we assume the minimum measured $^{36}\text{Ar}/^{37}\text{Ar}$ ratio represents pure $^{36}\text{Ar}_{\text{cos}}$ and subtract out any trapped ^{36}Ar using this value (Garrison et al. 2000), the isochron normalized to $^{36}\text{Ar}_{\text{cos}}$ gives an age of 170 ± 14 Ma, in agreement with the age obtained by normalizing to ^{37}Ar . The isochron constructed by normalization to total ^{36}Ar shows more scatter and gives an age of 148 ± 53 Ma. All of these ages were calculated using the Williamson (1968) technique, which weighs each isotopic ratio by its uncertainty. These isochron ages and intercept ratios are summarized in Table 1. All of these Plag isochron ages lie within uncertainties of the Sm-Nd and Rb-Sr age for Los Angeles. This indicates that we have successfully resolved trapped Martian ^{40}Ar (represented by the $^{40}\text{Ar}/^{37}\text{Ar}$ intercept) from $^{40}\text{Ar}^*$ arising from in situ decay. The positive intercept of these isochrons indicate that this trapped ^{40}Ar resided throughout the Plag lattice (see Appendix 2).

For Los Angeles WR, the $^{36}\text{Ar}/^{37}\text{Ar}$ ratios decrease steadily to 80% ^{39}Ar release, consistent with the release of substantial amounts of trapped ^{36}Ar , then remain constant to within a few percent. Figure 3 plots the $^{40}\text{Ar}/^{37}\text{Ar}$ and $^{39}\text{Ar}/^{37}\text{Ar}$ ratios for 37–100% ^{39}Ar release, which are those extractions showing increasing age above the Plag age, and compares these to a hypothetical isochron passing through zero and representing a formation age of 170 Ma. The WR data all plot well above the hypothetical isochron and do not define a particular linear trend. Those extractions releasing

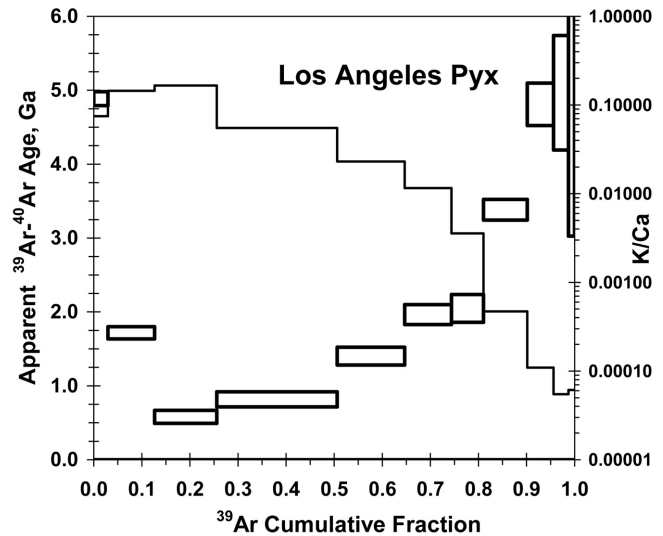


Fig. 4. ^{39}Ar - ^{40}Ar age spectrum (rectangles, left y-axis) and K/Ca ratios (stepped line, right y-axis) as a function of cumulative ^{39}Ar release for Los Angeles Pyx.

57–100% of the ^{39}Ar data (15 of 17 plotted points) are moderately linear, and a best fit line through these gives an “age” of 343 ± 4 Ma and a positive intercept. As an alternate approach, we also assumed Los Angeles WR contained a concentration of $^{36}\text{Ar}_{\text{cos}}$ equal to that observed in some other basaltic shergottites ($\sim 2 \times 10^{-9} \text{ cm}^3/\text{g}$) and used the $^{36}\text{Ar}/^{37}\text{Ar}$ ratio to subtract $^{36}\text{Ar}_{\text{cos}}$ from all extractions (Garrison et al. 2000). A best fit line for 37–100% ^{39}Ar and normalized to trapped ^{36}Ar gives an unweighed “age” of 291 ± 12 Ma and a $^{40}\text{Ar}/^{36}\text{Ar}$ intercept ratio of 187 ± 10 . In all of these WR “isochrons,” including those data releasing 0–37% of the ^{39}Ar substantially increases scatter in the data. We conclude that these derived isochron ages are not real and that excess ^{40}Ar was released in significant amounts from phases with different K/Ca ratios for all these WR extractions (see Appendix 2).

The Ar-Ar age spectrum for Los Angeles Pyx (Fig. 4) has large uncertainties, due to the very low K concentration, which produced both significant blank and reactor corrections. Higher $^{36}\text{Ar}/^{37}\text{Ar}$ ratios for the first two extractions indicate adsorbed terrestrial Ar. K/Ca ratios (~ 0.1) for the early extractions resemble those for the Plag and WR and probably reflect plagioclase contamination in the Pyx separate. The K/Ca of later extractions decreases by several orders of magnitude and reflect increasing Ar degassing from pyroxene. The age greatly increases in these later extractions, indicating substantial trapped Martian ^{40}Ar residing in pyroxene. Isochron plots for these data show too much scatter to be meaningful.

NWA 3171

The Ar-Ar age spectrum for NWA 3171 Plag is shown in Fig. 5. The preliminary Sm-Nd isochron age for NWA 3171 is

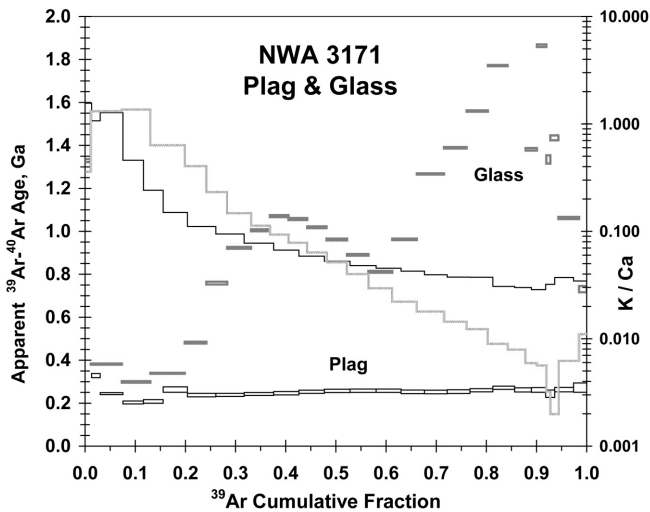


Fig. 5. ^{39}Ar - ^{40}Ar age spectra (rectangles, left Y-axis) and K/Ca ratios (stepped lines, right Y-axis) as a function of cumulative ^{39}Ar release for Plag (sharp lines) and Glass (fuzzy lines) samples of NWA 3171. Age uncertainties ($\sim 1\sigma$) are represented by the width of the rectangles.

193 ± 21 Ma (Nyquist et al. 2008, personal communication). For the first 20% of the ^{39}Ar release of the Plag, variable ages, high K/Ca ratios (compared to other extractions), and high $^{36}\text{Ar}/^{37}\text{Ar}$ ratios that decrease by three orders of magnitude over the extractions all indicate terrestrial weathering of grain surfaces (Appendix 2). Such weathering is commonly observed in hot desert meteorites. Above 20% ^{39}Ar release, the ages steadily increase from ~ 0.24 Ga to ~ 0.26 Ga (average age of 0.254 Ga), and the K/Ca decreases from ~ 0.1 to ~ 0.03 . The $^{36}\text{Ar}/^{37}\text{Ar}$ ratios for these extractions are relatively constant, suggesting that ^{36}Ar is mostly cosmogenic in origin. Assuming the minimum measured $^{36}\text{Ar}/^{37}\text{Ar}$ ratio represents pure $^{36}\text{Ar}_{\text{cos}}$ and calculating the total $^{36}\text{Ar}_{\text{cos}}$ gives 1.5×10^{-9} cm^3/g , a value slightly lower than typical $^{36}\text{Ar}_{\text{cos}}$ measured for some basaltic shergottites (Eugster et al. 1997; Terribilini et al. 1998; Schwenzer et al. 2007; Eugster et al. 2002; Park 2005). Cosmogenic Ar has not yet been reported for unirradiated NWA 3171. As little trapped ^{36}Ar likely was released above 20% ^{39}Ar , we examined isochron plots for these data by normalizing both to ^{37}Ar and to total ^{36}Ar . The ratios normalized to ^{37}Ar have the smaller uncertainties and are shown in Fig. 6, along with a hypothetical isochron representing the formation age of 193 Ma. The Plag isochron age normalized to ^{37}Ar is 232 ± 7 Ma. The isochron age normalized to total ^{36}Ar is identical but less precise, 229 ± 28 Ma. Both of these ages were calculated using the Williamson (1968) technique to weigh individual ratios by their uncertainties. Within uncertainties, these Ar-Ar isochron ages are only slightly higher than the Sm-Nd formation age. The intercept ratios of both these isochrons (Table 1) are positive and suggest that a trapped ^{40}Ar component, located throughout the lattice, was separated from $^{40}\text{Ar}^*$ (see Appendix 2).

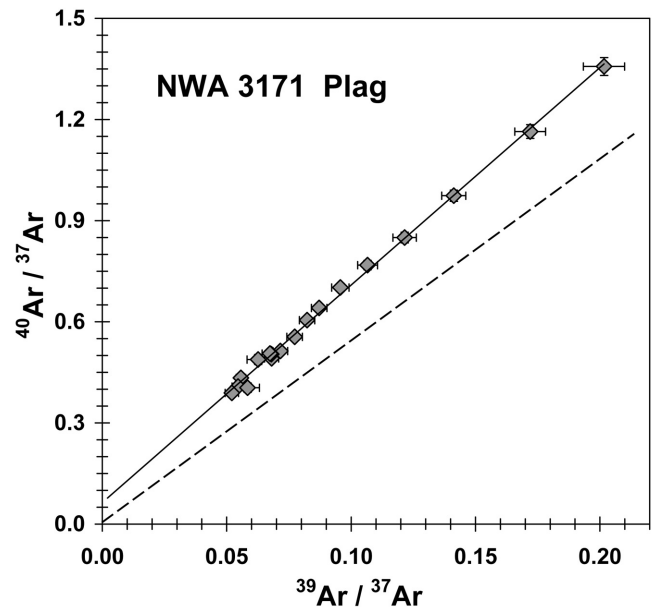


Fig. 6. Plot of $^{40}\text{Ar}/^{37}\text{Ar}$ versus $^{39}\text{Ar}/^{37}\text{Ar}$ for 20–100% ^{39}Ar release of NWA 3171 Plag. Individual ratio uncertainties are indicated or are smaller than plotted symbols. A hypothetical isochron through the origin and representing a formation age of 193 Ma is shown by the dashed line.

The Ar-Ar age spectrum for NWA 3171 Glass (Fig. 5) shows much more variable ages compared to the Plag and clearly reveals significant amounts of trapped Martian ^{40}Ar . At low extraction temperatures the ages resemble those for the Plag, then rise to ~ 1.1 Ga at $\sim 40\%$ ^{39}Ar release and to ~ 1.9 Ga at 90% ^{39}Ar release. To evaluate $^{40}\text{Ar}_{\text{xs}}$ in the Glass, we utilize a plot of $^{36}\text{Ar}_{\text{trap}}/^{40}\text{Ar}$ versus $^{39}\text{Ar}/^{40}\text{Ar}$ (Fig. 7). This type of plot works best in situations where trapped ^{40}Ar dominates over $^{40}\text{Ar}^*$ from in situ decay (Bogard and Garrison 1999). The Sm-Nd age of NWA 3171 defines a point on the $^{39}\text{Ar}/^{40}\text{Ar}$ axis and the data define mixing lines between the $^{40}\text{Ar}^*$ arising from in situ decay and $^{36}\text{Ar}_{\text{trap}}/^{40}\text{Ar}$. The $^{36}\text{Ar}/^{37}\text{Ar}$ ratios of the Glass are variable, and we have no accurate way to determine the $^{36}\text{Ar}_{\text{cos}}$ concentration. Thus, we selected a value for $^{36}\text{Ar}_{\text{cos}}$ (2.5×10^{-9} cm^3/g) that minimized the scatter in those data releasing most of the trapped Ar, which is a reasonable approach if trapped Ar is a single component. This $^{36}\text{Ar}_{\text{cos}}$ is only slightly higher than $^{36}\text{Ar}_{\text{cos}}$ measured in some other basaltic shergottites with similar formation ages (Eugster et al. 1997; Terribilini et al. 1998; Park et al. 2003; Park 2005; Schwenzer et al. 2007;). The lower temperature extractions scatter (Fig. 7) and are consistent with varying degrees of diffusive loss of $^{40}\text{Ar}^*$, adsorbed terrestrial Ar, and mobility of K during terrestrial weathering. Those extractions releasing 33–93% of the ^{39}Ar , however, define a tight cluster on a mixing line between an age of ~ 193 Ma and a trapped Martian component with a $^{40}\text{Ar}/^{36}\text{Ar}$ ratio of ~ 1700 . If we assume $^{36}\text{Ar}_{\text{cos}}$ is similar to that in some other shergottites (2.0×10^{-9} cm^3/g) trapped $^{40}\text{Ar}/^{36}\text{Ar}$ becomes ~ 1400 , but the data scatter increase. The

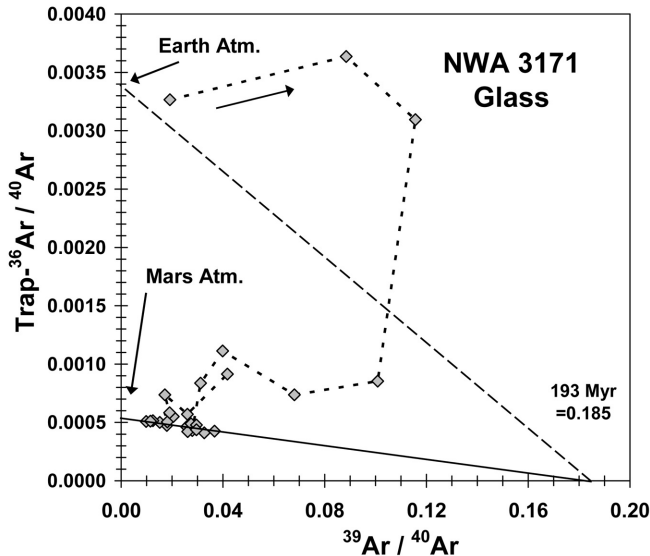


Fig. 7. Plot of $^{36}\text{Ar}/^{40}\text{Ar}$ versus $^{39}\text{Ar}/^{36}\text{Ar}$, where ^{36}Ar is a calculated trapped component, for all extractions of NWA 3171 glass. The dotted line and arrow indicate the progression of extraction temperatures, with the lowest temperature near the terrestrial composition. The dashed and solid lines represent mixtures between $^{40}\text{Ar}^*$ from in situ decay and the terrestrial and Martian atmospheres, respectively.

minimum measured $^{36}\text{Ar}/^{37}\text{Ar}$ defines a maximum trapped $^{40}\text{Ar}/^{36}\text{Ar}$ of ~ 2050 . These trapped ratios are similar to values of trapped Martian atmosphere reported in some other Martian meteorites (Bogard and Garrison 1999; Walton et al. 2007). We conclude that NWA 3171 Glass mainly contains shock-implanted Martian atmosphere, which is not obviously present in NWA 3171 Plag.

NWA 2975

The Ar-Ar age spectrum for NWA 2975 Plag (Fig. 8) is erratic, and all ages are older than the Sm-Nd age of 177 ± 11 Ma (Nyquist et al. 2008, personal communication). As the extraction proceeded, the $^{36}\text{Ar}/^{37}\text{Ar}$ ratio decreased by two orders of magnitude, indicating early release of a significant trapped ^{36}Ar component. Trapped Ar released at the lowest temperatures possibly is terrestrial, but trapped Ar released at intermediate and higher temperatures is probably Martian. Assuming the minimum measured $^{36}\text{Ar}/^{37}\text{Ar}$ ratio (at 1250°C) represents pure $^{36}\text{Ar}_{\text{cos}}$, the calculated total $^{36}\text{Ar}_{\text{cos}}$ is 2.2×10^{-9} cm^3/g , a value similar to $^{36}\text{Ar}_{\text{cos}}$ measured for other basaltic shergottites (Eugster et al. 1997; Terribilini et al. 1998; Eugster et al. 2002; Park 2005; Schwenger et al. 2007). A plot of $^{40}\text{Ar}/^{37}\text{Ar}$ versus $^{39}\text{Ar}/^{37}\text{Ar}$ for 12–100% ^{39}Ar release (Fig. 9) gives a weighed isochron “age” of 672 ± 8 Ma and suggests a small negative intercept. Some isochron rotation may have occurred due to ^{39}Ar recoil or preferential release of $^{40}\text{Ar}_{\text{xs}}$ at lower temperatures (see Appendix 2). We also used the minimum measured $^{36}\text{Ar}/^{37}\text{Ar}$ ratio to calculate trapped

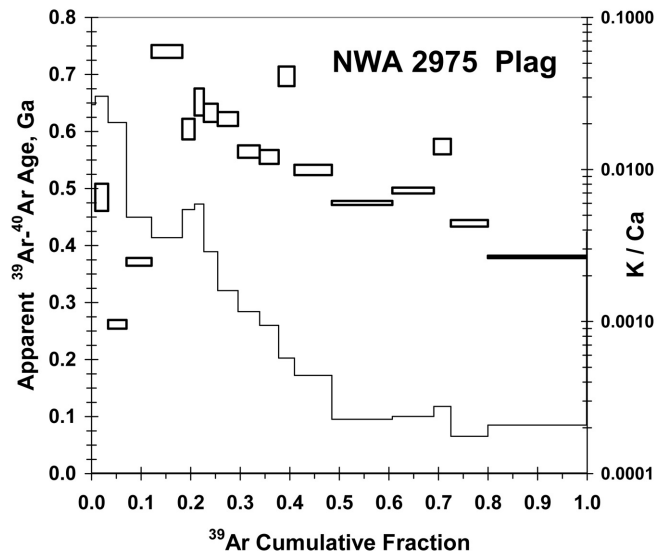


Fig. 8. ^{39}Ar - ^{40}Ar age spectrum (rectangles, left Y-axis) and K/Ca ratios (stepped line, right Y-axis) as a function of cumulative ^{39}Ar release from NWA 2975 Plag.

^{36}Ar for each extraction. The isochron for 18–100% ^{39}Ar release and normalized to trapped ^{36}Ar gives an “age” of 366 ± 3 Ma and a positive $^{40}\text{Ar}/^{36}\text{Ar}$ intercept of 816 ± 19 . These two ages, which differ significantly from each other and from the Sm-Nd age, are not real. The significant spread in K/Ca ratios and the observation that most extractions show $^{40}\text{Ar}_{\text{xs}}$, indicate that most $^{40}\text{Ar}_{\text{xs}}$ is contained in K-bearing portions of the lattice (see Appendix 2).

Dhofar 019

The Ar-Ar age spectrum for Dho 019 Plag and WR (Fig. 10) both begin at elevated ages, which then decrease to values of ~ 0.7 Ga. Higher ages and $^{36}\text{Ar}/^{37}\text{Ar}$ ratios for the first few extractions probably represent terrestrial weathering of grain surfaces, especially of the WR. Nine extractions of the Plag, releasing 15–100% of the ^{39}Ar , give an average plateau age of 655 ± 38 Ma. The Sm-Nd isochron age for Dho 019 is 575 ± 7 Ma (Borg et al. 2001). Beyond the first few extractions of both Plag and WR, the $^{36}\text{Ar}/^{37}\text{Ar}$ ratios are relatively constant, and most ^{36}Ar released is probably cosmogenic. Thus, a trapped ^{36}Ar component cannot be calculated. We calculate $^{36}\text{Ar}_{\text{cos}}$ concentrations of 1.5×10^{-8} cm^3/g and $\sim 1.3 \times 10^{-8}$ cm^3/g for the Plag and WR, respectively. Although these values are much larger than those of other shergottites, the Dho 019 cosmic ray exposure (CRE) age is much older, ~ 20 Ma, and the reported $^{36}\text{Ar}_{\text{cos}}$ for non-irradiated Dho 019 is about 1.1×10^{-8} $\text{cm}^3\text{STP/g}$ (Shukolyukov et al. 2002; Park 2005).

Figure 11 plots $^{40}\text{Ar}/^{37}\text{Ar}$ versus $^{39}\text{Ar}/^{37}\text{Ar}$ for Plag extractions releasing 15–100% of the ^{39}Ar , and for WR extractions releasing 33–100% of the ^{39}Ar . Including lower temperature data in these plots significantly increases the

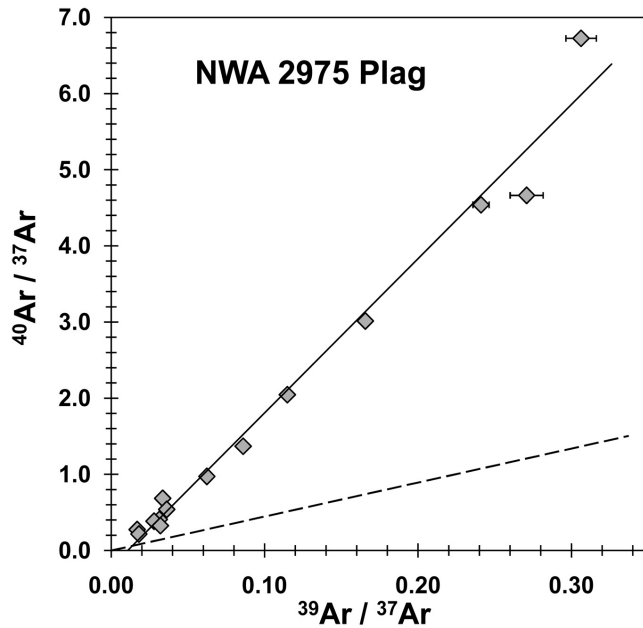


Fig. 9. Plot of $^{40}\text{Ar}/^{37}\text{Ar}$ versus $^{39}\text{Ar}/^{37}\text{Ar}$ for extractions releasing 12–100% of the ^{39}Ar from NWA 2975 Plag. Individual ratio uncertainties are indicated or are smaller than plotted symbols. A hypothetical isochron through the origin and representing a formation age of 177 Ma is shown by the dashed line.

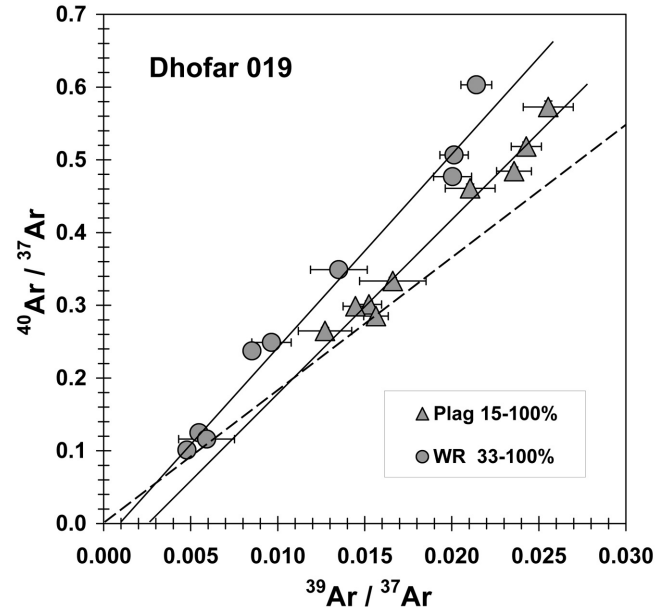


Fig. 11. Plot of $^{40}\text{Ar}/^{37}\text{Ar}$ versus $^{39}\text{Ar}/^{37}\text{Ar}$ for extractions releasing 15–99.9% of the ^{39}Ar for Dho 019 Plag (triangles) and 33–99.9% of the ^{39}Ar for Dho 019 WR (circles). Individual ratio uncertainties are indicated or are smaller than plotted symbols. A hypothetical isochron through the origin and representing a formation age of 575 Ma is shown by the dashed line.

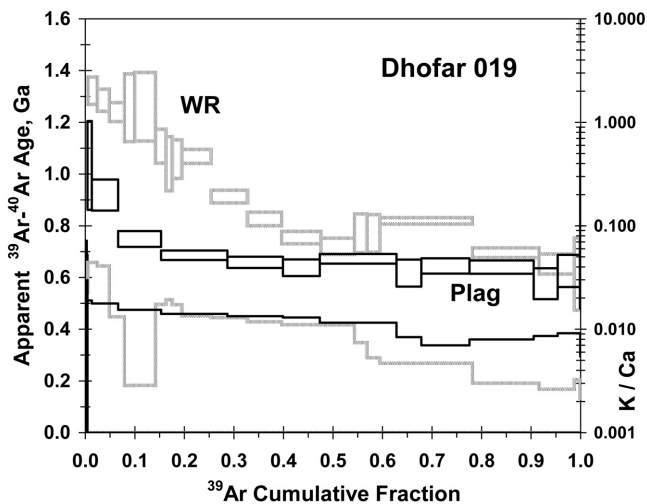


Fig. 10. ^{39}Ar - ^{40}Ar age spectra (rectangles, left Y-axis) and K/Ca ratios (stepped line, right Y-axis) as a function of cumulative ^{39}Ar release for Plag (sharp lines) and WR (fuzzy lines) samples of Dho 019.

scatter. All points plot near or slightly above the hypothetical 575 Ma isochron through the origin and indicate the presence of $^{40}\text{Ar}_{\text{xs}}$. For Plag, the weighed isochron “age” is 721 ± 41 Ma and the intercept is -0.047 ± 0.031 . For WR, the weighed isochron “age” is 849 ± 25 Ma and the intercept is -0.028 ± 0.009 . The same Plag data normalized to total ^{36}Ar shows somewhat greater scatter but give a similar “age” of $710 \pm$

72 Ma. The negative intercepts suggest some isochron rotation may have occurred (see Appendix 2). Because there is no indication of gain of recoiled ^{39}Ar at highest extraction temperature, any rotation likely was caused by preferential release of $^{40}\text{Ar}_{\text{xs}}$ at lower temperatures, as also is indicated by Fig. 10. We also used the minimum measured $^{36}\text{Ar}/^{37}\text{Ar}$ ratio to calculate $^{36}\text{Ar}_{\text{cos}}$ concentrations for each Plag extraction releasing 0.1–15% of the ^{39}Ar . A weighed isochron of these data, normalized to trapped ^{36}Ar , gives an “age” of 707 ± 16 Ma and a higher intercept of 165 ± 43 . Both the age spectra and isochron ages are higher than the Sm-Nd age, and the meteorite obviously released trapped Martian ^{40}Ar from both Plag and WR.

DaG 476

The Ar-Ar age spectra for WR and Plag samples are given in Fig. 12, and for light (Mg-rich) and dark (Fe-rich) pyroxene separates in Fig. 13. The Sm-Nd age of DaG 476 is 474 ± 11 Ma (Borg et al. 2003). All Ar-Ar spectra are complex and indicate the significant presence of trapped ^{40}Ar . Our DaG 476 sample exhibited some terrestrial weathering, and all four samples showed higher values of the $^{36}\text{Ar}/^{37}\text{Ar}$ ratios for the first few extractions. Terrestrial ^{40}Ar could have been a significant part of the total ^{40}Ar released for the first ~18% and 24% of the WR and Plag, respectively, and for the first ~12–19% of the two Pyx samples. However, compared to these extractions, ratios of $^{36}\text{Ar}/^{37}\text{Ar}$ were considerably lower

and somewhat constant for higher temperature extractions of all samples, which probably indicate trapped ^{40}Ar released in these extractions is Martian. Adopting the lowest measured $^{36}\text{Ar}/^{37}\text{Ar}$ ratio in the Plag as representing pure $^{36}\text{Ar}_{\text{cos}}$, the total calculated $^{36}\text{Ar}_{\text{cos}}$ in the Plag, $1.9 \times 10^{-9} \text{ cm}^3/\text{g}$, is similar to $^{36}\text{Ar}_{\text{cos}}$ in basaltic shergottites (Eugster et al. 1997; Terribilini et al. 1998; Eugster et al. 2002; Park 2005; Schwenzer et al. 2007). Reported cosmogenic ^{36}Ar for non-irradiated DaG 476 WR samples is $0.65 \times 10^{-9} \text{ cm}^3\text{STP/g}$ (Park 2005). Because $^{36}\text{Ar}_{\text{cos}}$ is primarily produced from Ca, whose concentration differs between DaG 476 Pyx samples and DaG 476 Plag and basaltic shergottites, calculated $^{36}\text{Ar}_{\text{cos}}$ in the Pyx samples are lower than in the Plag. Consequently, we examined isochron plots normalized to both ^{37}Ar and total ^{36}Ar for these higher temperature data. (Trapped ^{36}Ar cannot be resolved.) These isochrons for all four DaG samples (not shown) show significant scatter and do not give meaningful ages. These isochron plots, as well as the Ar-Ar age spectra, suggest the presence of significant amounts of trapped Martian ^{40}Ar .

NWA 1068

The Ar-Ar age spectrum of NWA 1068 WR (Fig. 14) falls to a minimum age of $61 \pm 3 \text{ Ma}$ over 12–25% ^{39}Ar release, then increases, with the age increase accelerating above 90% ^{39}Ar release, where rapidly decreasing K/Ca ratios indicate pyroxene is degassing. The Sm-Nd age of NWA 1068 is $185 \pm 11 \text{ Ma}$ (Shih et al. 2003). The very young Ar-Ar age and high but decreasing $^{36}\text{Ar}/^{37}\text{Ar}$ and K/Ca ratios for the first few extractions indicate terrestrial weathering with concurrent loss of $^{40}\text{Ar}^*$ (see Appendix 2). Relatively constant $^{36}\text{Ar}/^{37}\text{Ar}$ ratios above 42% ^{39}Ar release suggest mostly $^{36}\text{Ar}_{\text{cos}}$ was released, in an amount, $\sim 1.7 \times 10^{-9} \text{ cm}^3/\text{g}$, similar to $^{36}\text{Ar}_{\text{cos}}$ measured in a non-irradiated NWA 1068 sample ($1.56 \times 10^{-9} \text{ cm}^3\text{STP/g}$; Mathew et al. 2003). Isochron plots of extractions releasing 42–100% ^{39}Ar , normalized to either ^{37}Ar or total ^{36}Ar , scatter considerably. As with Dho 019, the implication is that NWA 1068 released significant amounts of trapped ^{40}Ar from both plagioclase and pyroxene.

Y-980459 and SaU 005

The Ar-Ar age spectra for whole rock samples of olivine phyric shergottites Y-980459 and SaU 005 (Fig. 15) are complex and also indicate the presence of $^{40}\text{Ar}_{\text{xs}}$. The Sm-Nd ages of Y-980459 and SaU 005 are $472 \pm 47 \text{ Ma}$ (Shih et al. 2005) and $445 \pm 18 \text{ Ma}$ (Shih et al. 2007), respectively. Four of five extractions releasing 44–94% of the ^{39}Ar from Y-980459 give very similar ages having an average value of $866 \pm 35 \text{ Ma}$. Higher $^{36}\text{Ar}/^{37}\text{Ar}$ and K/Ca ratios for the first four extractions of Y-980458 (0–17% ^{39}Ar) suggest release of terrestrial Ar, but $^{36}\text{Ar}/^{37}\text{Ar}$ for the remaining extractions are relatively constant. Adopting the minimum

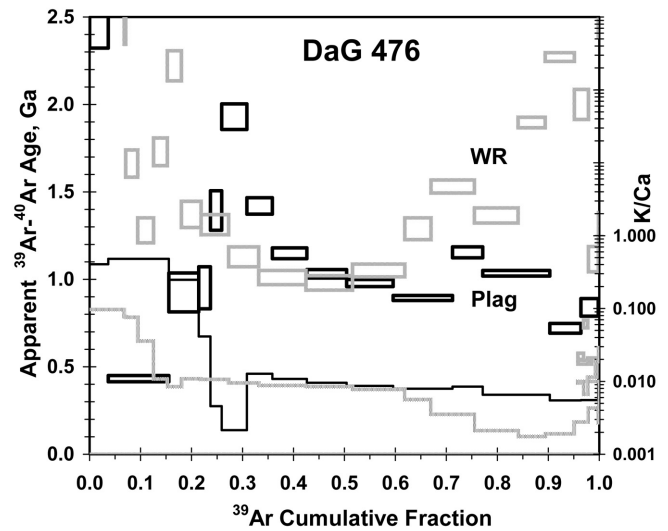


Fig. 12. ^{39}Ar - ^{40}Ar age spectra (rectangles, left Y-axis) and K/Ca ratios (stepped lines, right Y-axis) as a function of cumulative ^{39}Ar release for Plag (sharp lines) and WR (fuzzy lines) samples of DaG 476.

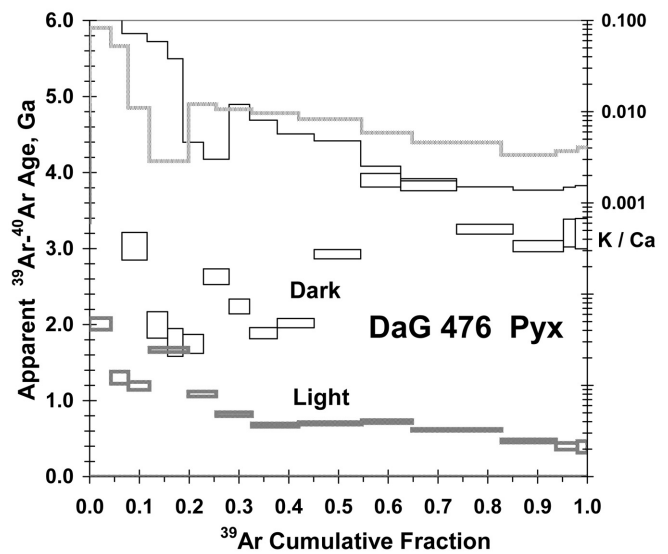


Fig. 13. ^{39}Ar - ^{40}Ar age spectra (rectangles, left Y-axis) and K/Ca ratios (stepped lines, right Y-axis) as a function of cumulative ^{39}Ar release for Light and Dark Pyx samples of DaG 476.

measured $^{36}\text{Ar}/^{37}\text{Ar}$ ratio to calculate total $^{36}\text{Ar}_{\text{cos}}$ for Y-980459 gives $1.3 \times 10^{-9} \text{ cm}^3/\text{g}$, a value similar to reported cosmogenic ^{36}Ar of $1.5 \times 10^{-9} \text{ cm}^3\text{STP/g}$ in an unirradiated WR sample (Okazaki and Nagao 2004; Christen et al. 2005). This suggests that mostly $^{36}\text{Ar}_{\text{cos}}$ and Martian ^{40}Ar were released above 17% ^{39}Ar release. An isochron plot of those Y-980459 extractions releasing 30–100% of the ^{39}Ar and normalized to ^{37}Ar scatters considerably and does not define an isochron.

The $^{36}\text{Ar}/^{37}\text{Ar}$ ratios for SaU 005 WR remain high through $\sim 27\%$ of the ^{39}Ar release, whereas $^{36}\text{Ar}/^{37}\text{Ar}$ ratios

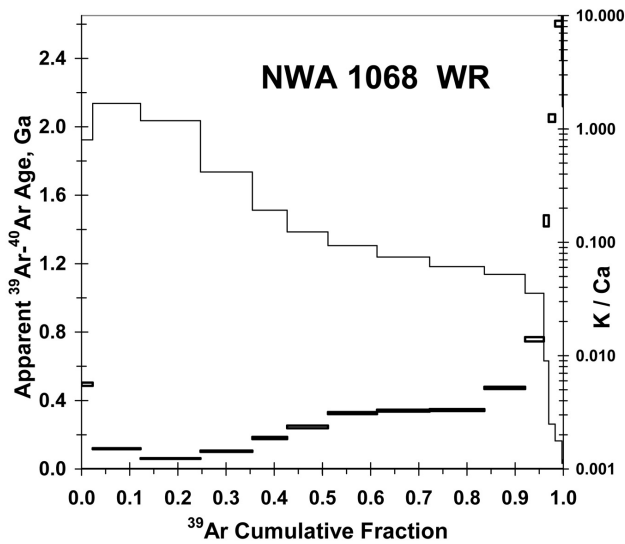


Fig. 14. ^{39}Ar - ^{40}Ar age spectrum (rectangles, left Y-axis) and K/Ca ratios (stepped line, right Y-axis) as a function of cumulative ^{39}Ar release for NWA 1068 WR.

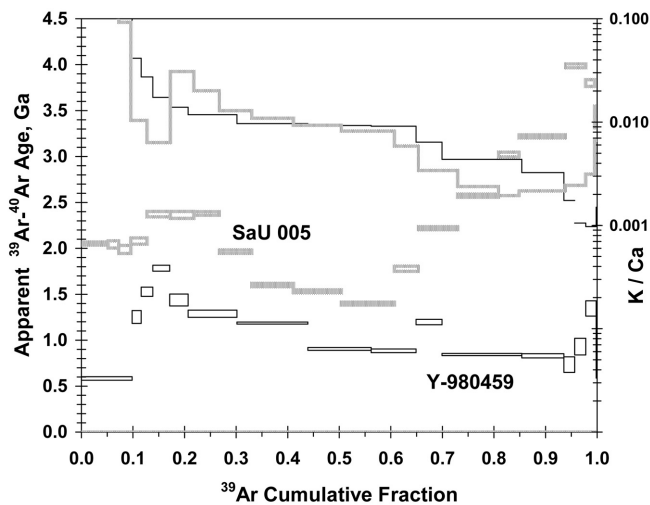


Fig. 15. ^{39}Ar - ^{40}Ar age spectra (rectangles, left Y-axis) and K/Ca ratios (stepped lines, right Y-axis) as a function of cumulative ^{39}Ar release for WR samples of Y-980459 and SaU 005.

for the remaining extractions are somewhat constant. Using the minimum measured $^{36}\text{Ar}/^{37}\text{Ar}$ to calculate total $^{36}\text{Ar}_{\text{cos}}$ gives a value of $1.9 \times 10^{-9} \text{ cm}^3/\text{g}$. This value is larger than WR $^{36}\text{Ar}_{\text{cos}}$ of $0.58 \times 10^{-9} \text{ cm}^3/\text{STP/g}$ measured in unirradiated samples (Eugster et al. 2002; Mathew et al. 2003; Park 2005). The average CRE age for SaU 005 is $1.2 \pm 0.3 \text{ Ma}$ (Eugster et al. 2002 and the references therein). These observations indicate that higher Ar-Ar ages for the early extractions were produced by the release of terrestrial ^{40}Ar from weathered phases, and that mainly Martian ^{40}Ar and $^{36}\text{Ar}_{\text{cos}}$ were released at higher temperatures. However, an isochron plot of these data normalized to ^{37}Ar shows considerable scatter and does not define an isochron.

ARGON CONCENTRATIONS

Trapped ^{40}Ar and Cosmogenic ^{36}Ar

Virtually all Ar-Ar analyses of shergottites indicate the presence of excess Martian ^{40}Ar beyond amounts expected to accumulate by in situ decay of ^{40}K since formation of the individual meteorites, as defined by their Sm-Nd and/or Rb-Sr isochron ages. In most cases not even argon isochron plots fully resolve $^{40}\text{Ar}^*$ from trapped Martian ^{40}Ar , and sometimes this $^{40}\text{Ar}_{\text{xs}}$ resides in more than one mineral site within the lattice (Appendix 2). For the data discussed above, only Los Angeles Plag and possibly NWA 3171 Plag give Ar-Ar isochron ages within uncertainties of the meteorite formation age determined by other chronometers. In this section we calculate for each shergottite analysis the concentration of trapped Martian ^{40}Ar in excess of that arising from in situ decay. To do so, we must estimate the amount of adsorbed terrestrial atmospheric ^{40}Ar and calculate the $^{40}\text{Ar}^*$ from in situ ^{40}K decay since the formation age, then subtract both from the total measured ^{40}Ar . Below we examine the mechanism of and uncertainties in these corrections. Table 2 summarizes the formation ages utilized and results of these calculations.

We calculated the amount of $^{40}\text{Ar}^*$ accumulating from in situ decay since meteorite formation by identifying the $^{40}\text{Ar}^*/^{39}\text{Ar}$ ratio for each sample that gives its formation age and summing the $^{40}\text{Ar}^*$ concentration across all extractions. We did not calculate directly from the K concentrations determined for these samples (Table 2), as that would involve an extra uncertainty arising from determining the K concentration. For many samples with low K concentration, calculated $^{40}\text{Ar}^*$ is a very minor part of total measured ^{40}Ar . For Plag and some WR samples, calculated $^{40}\text{Ar}^*$ is a larger fraction of total ^{40}Ar and will depend somewhat on the formation age utilized. For those reported formation ages having uncertainties of only a few Ma, at most a very few percent uncertainty exists in calculated $^{40}\text{Ar}^*$. However, it is not clear whether those shergottite ages ranging over 165–193 Ma (Table 2) really differ in age or have the same formation age. Assuming a formation age for Los Angeles of 190 Ma, rather than the 170 Ma used, changes the calculated $^{40}\text{Ar}^*$ from 2.20 to $2.46 \times 10^{-6} \text{ cm}^3/\text{g}$, a 12% increase. Thus, in determining trapped Martian ^{40}Ar in these meteorites, uncertainties in calculating some $^{40}\text{Ar}^*$ concentrations may be $\sim 10\%$ and may explain part of the variation in trapped Martian ^{40}Ar among different samples.

Evidence for terrestrial ^{40}Ar degassing in the first few extractions of some of these analyses include a rapid decrease in $^{36}\text{Ar}/^{37}\text{Ar}$ ratio, an anomalously high K/Ca ratio, and an anomalously high initial Ar-Ar age, suggesting adsorption of terrestrial atmospheric Ar. We subtracted the minimum measured $^{36}\text{Ar}/^{37}\text{Ar}$ from the measured $^{36}\text{Ar}/^{37}\text{Ar}$ for each extraction (Garrison et al. 2000) in order to get an estimate of cosmogenic ^{36}Ar (Table 2) and then summed these across

Table 2. Concentrations of ^{40}Ar (10^{-7} cm³/g) and $^{36}\text{Ar}_{\text{cos}}$ (10^{-9} cm³/g).

| Meteorite/phase | K (ppm) | ^{40}Ar total | ^{40}Ar Martian | $^{40}\text{Ar}^*$ decay | ^{40}Ar excess | $^{36}\text{Ar}_{\text{cos}}$ here | Lit. |
|-------------------------------------|---------|------------------------|--------------------------|--------------------------|-------------------------|------------------------------------|---|
| New Data | | | | | | | |
| Los Angeles , 170 ± 8 Ma (a) | | | | | | | |
| Plag | 2804 | 33.4 | 30.5 | 22 | 8.5 | 2.8 | <i>2.5–3.2 (m,n,o)</i> |
| WR | 1802 | 27.2 | 26.1 | 11.9 | 14.2 | 3.4 | |
| Pyx | 45 | 11.3 | 9.52 | 0.36 | 9.16 | 4.3 | |
| NWA 3171 , 193 ± 21 Ma (b) | | | | | | | |
| Plag | 3745 | 45.3 | 35.8 | 27.3 | 8.5 | 2.6 | <i>n.a.</i> |
| Melt | 1478 | 76.6 | 73.4 | 10.9 | 62.5 | 3 | |
| NWA 2975 , ~177 ± 11 Ma (c) | | | | | | | |
| Plag | 884 | 18.7 | 18 | 5.8 | 12.3 | 2.2 | <i>n.a.</i> |
| NWA 1068 , 182 ± 11 Ma (d) | | | | | | | |
| WR | 1426 | 24 | 23.3 | 10 | 13.2 | 2 | <i>1.6 (p)</i> |
| Dho 019 , 575 ± 7 Ma (h) | | | | | | | |
| Plag | 1016 | 35.8 | 26.9 | 17.7 | 9.2 | 15 | <i>11 (o,q)</i> |
| WR | 421 | 26.2 | 23.9 | 9.1 | 14.8 | 12 | |
| DaG 476 , 474 ± 11 Ma (i) | | | | | | | |
| Plag | 490 | 26.7 | 22.6 | 9.5 | 13.1 | 1.9 | <i>0.53–0.77 (o)</i> |
| WR | 158 | 32.2 | 13.4 | 3.2 | 10.2 | 1.3 | |
| Pyx-Lt | 219 | 9.5 | 8.6 | 4.2 | 4.4 | 1.1 | |
| Pyx-Dk | 90 | 56.3 | 26.7 | 1.7 | 24.9 | 1.6 | |
| Y-980459 , 472 ± 47 Ma (j) | | | | | | | |
| WR | 148 | 7.7 | 7.3 | 2.8 | 4.5 | 1.3 | <i>1.5 (r,s)</i> |
| SaU 005 , 445 ± 18 Ma (k) | | | | | | | |
| WR | 570 | 31.3 | 30.2 | 3.2 | 26.9 | 1.9 | <i>0.38–0.80 (n,o,p)</i> |
| Literature Data | | | | | | | |
| Zagami , 166 ± 6 Ma (a, g) | | | | | | | |
| CG Plag | 4894 | 50 | 49 | 34.2 | 15.8 | 1.9 | <i>(see footnote)</i> <i>1.5–1.9</i> |
| FG Plag | 2917 | 47.4 | 43.1 | 19.8 | 23.4 | 2 | |
| CG Pyx2 | 270 | 13.7 | 12.6 | 1.8 | 10.8 | 2.5 | <i>1.8–2.6</i> |
| FG Pyx2 | 226 | 12.1 | 10.7 | 1.5 | 9.2 | 2.4 | |
| FG Pyx1 | 281 | 20.2 | 17.2 | 1.9 | 15.3 | 2.9 | |
| Shergotty , 165 ± 4 Ma (a) | | | | | | | |
| WR | 1725 | 31.9 | 27.2 | 10.5 | 16.7 | 2.7 | <i>(see footnote)</i> |
| WR | 1810 | | 37.9 | | | | |
| Feld | 3440 | | 45.2 | | | | |
| Pyx | 175 | | 20.5 | | | | |
| QUE 94201 , 327 ± 10 Ma (l) | | | | | | | |
| Plag | 329 | 16.5 | 9.3 | 4.6 | 4.7 | 0.85 | |
| Y-793605 , 185 ± 16 Ma (f) | | | | | | | |
| WR | 124 | 18.3 | 18 | 0.9 | 17.1 | 2.3 | <i>1.1–1.6 (t,u)</i> |
| Y-000097 , ~189 ± 18 Ma (e) | | | | | | | |
| Plag | 1850 | 19.9 | 19.9 | 10 | 9.9 | 2.3 | <i>1.4 (v)</i> |

The first column gives the meteorite name, and beneath that, the meteorite phases analyzed. The formation age and reference is given after the meteorite name. Other columns (left to right) give determined K concentration, total measured ^{40}Ar , total Martian ^{40}Ar derived by subtracting terrestrial ^{40}Ar (see text), $^{40}\text{Ar}^*$ from in situ decay calculated from meteorite formation age, and trapped (excess) Martian ^{40}Ar . The last column gives for each of our samples an upper limit to cosmogenic ^{36}Ar calculated from Ar-Ar data, assuming the minimum measured $^{36}\text{Ar}/^{37}\text{Ar}$ ratio is a pure nuclear component. Values in italic in the last column after each meteorite name gives literature values (and source) of $^{36}\text{Ar}_{\text{cos}}$ concentrations

Sources of Ar-Ar literature data are Zagami from Bogard and Park (2008); Shergotty from Terribilini et al. (1998) and Bogard and Garrison 1999; Y-793605 and QUE 94201 from Bogard and Garrison 1999; Y-000097 from Misawa et al. 2008. Literature values for meteorite formation ages were reported by: (a) Nyquist et al. 2001a; (b) Nyquist et al., unpublished; (c) Nyquist et al. unpublished; (d) Shih et al. 2003; (e) Misawa et al. 2008; (f) Misawa et al. 2006a; (g) Borg et al. 2005; (h) Borg et al. 2001; (i) Borg et al. 2003; (j) Shih et al. 2005 (k) Shih et al. 2007, (l) Borg et al. 1997. Literature values of $^{36}\text{Ar}_{\text{cos}}$ concentration (10^{-9} cm³/g) were given in: (m) Garrison and Bogard 2000; (n) Eugster et al. 2002; (o) Park 2005; (p) Mathew et al. 2003; (q) Shukolyukov et al. 2002; (r) Okazaki and Nagao 2004; (s) Christen et al. 2005; (t) Nagao et al. 1997; (u) Terribilini et al. 1998; (v) Nagao et al. 2008. (n.a. = data not available). In addition, $^{36}\text{Ar}_{\text{cos}}$ literature values for Zagami and Shergotty are 1.8–2.6 for WR, 1.5–1.9 for Plag, and 1.8–2.6 for Pyx (Eugster et al. 1997; Terribilini et al. 1998; Park 2005; Schwenzer et al. 2007).

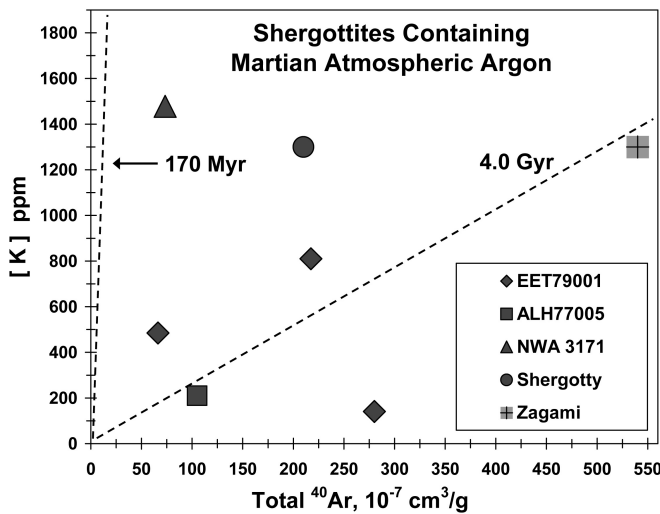


Fig. 16. Plot of total K versus total ^{40}Ar for shergottite samples containing Martian atmosphere Ar. The dashed lines indicate hypothetical isochrons. Sources of data are Elephant Moraine (EET) 79001, Allan Hills (ALH) 77005, and Shergotty (Garrison and Bogard 1998), NWA 3171 (glass sample, this work), and Zagami (Marti et al. 1995).

extractions. To identify terrestrial ^{40}Ar , we first assumed that all of the non-nuclear (trapped) ^{36}Ar in the first few extractions was terrestrial, and subtracted from total ^{40}Ar an amount of ^{40}Ar equal to 296 times the trapped ^{36}Ar . However, in several cases this gave a negative value for ^{40}Ar , indicating that part of the ^{36}Ar in these early extractions was Martian. In these cases, we reduced the assumed trapped $^{40}\text{Ar}/^{36}\text{Ar}$ ratio until a small positive value was obtained for the first extraction and used this ratio for any other corrections. This process may have over corrected for terrestrial ^{36}Ar and ^{40}Ar in some cases. However, our estimates of terrestrial ^{40}Ar are no greater than several percent for most samples (Table 2). As might be expected, atmospheric corrections were larger for some weathered, hot desert meteorites (e.g., DaG 476, Dho 019). In a very few cases we also omitted the ^{39}Ar in the first extraction as likely arising from terrestrial weathering, although in each case this omission was only a small fraction of the total ^{39}Ar . Total ^{39}Ar is used to calculate K concentration.

In the Results section we calculated for each shergottite a maximum concentration of $^{36}\text{Ar}_{\text{cos}}$ by assuming that the minimum measured $^{36}\text{Ar}/^{37}\text{Ar}$ ratio is a pure nuclear component. These maximum $^{36}\text{Ar}_{\text{cos}}$ values show reasonably good agreement with literature values for most samples (Table 2). Two basaltic shergottites for which $^{36}\text{Ar}_{\text{cos}}$ has not yet been reported (NWA 3171 and NWA 2975) have formation ages similar to Zagami and Shergotty and likely have similar CRE ages. Our maximum calculated $^{36}\text{Ar}_{\text{cos}}$ for these two NWA meteorites are also very similar to $^{36}\text{Ar}_{\text{cos}}$ reported for Zagami and Shergotty ($\sim 2 \times 10^{-9} \text{ cm}^3/\text{g}$; Table 2 footnote). This emphasizes the difficulty of constructing

isochron plots normalized to $^{36}\text{Ar}_{\text{trap}}$ and justifies our normalization of some isochron plots to total ^{36}Ar . Data for $^{36}\text{Ar}_{\text{cos}}$ in Table 2 also justifies our contention above that very little terrestrial atmosphere Ar was released from these samples at intermediate and high extraction temperatures. Because trapped ^{36}Ar usually dominates over $^{36}\text{Ar}_{\text{cos}}$ for the first few extractions, calculation of terrestrial ^{40}Ar is not very sensitive to the exact $^{36}\text{Ar}/^{37}\text{Ar}$ ratio used in the calculation.

We believe that K and trapped Martian ^{40}Ar concentrations given in Table 2 are accurate to within a few tens of percent. Concentrations of trapped Martian ^{36}Ar , and thus trapped Martian $^{40}\text{Ar}/^{36}\text{Ar}$ ratios, cannot be accurately determined. Most trapped Martian ^{40}Ar was released from these samples at higher temperatures, whereas much of the trapped ^{36}Ar was released at lower temperatures and is at least partly terrestrial contamination. Thus, the total trapped $^{40}\text{Ar}/^{36}\text{Ar}$ ratio tends to vary with temperature and is a mixture of different components.

Origin of Trapped Martian ^{40}Ar

The most striking aspect about the concentrations of trapped Martian ^{40}Ar given in Table 2 is that all samples show similar values of $\sim 10^{-6} \text{ cm}^3/\text{g}$. Similar $^{40}\text{Ar}_{\text{xs}}$ among different shergottites and mineral phases is not what one would expect if this excess ^{40}Ar derived from atmospheric ^{40}Ar implanted into small, shock melted inclusions. Such shock-melt phases are observed to be heterogeneously distributed in SNC meteorites, and thus shock-implanted Martian atmospheric gases would be expected to be highly variable in concentration among the different meteorites and mineral separates studied here. It also is unlikely that trapped ^{40}Ar in shergottites is Martian atmosphere adsorbed on Martian weathering products, as such Ar also would be expected to vary among meteorites and minerals and preferentially release at lower temperatures. Often, but not always, trapped Martian ^{40}Ar in shergottites preferentially releases at higher temperatures. Figure 16 illustrates the expected variability of Martian atmospheric ^{40}Ar by plotting total K versus total ^{40}Ar for several shergottite samples, including impact melts. (For the Zagami and Shergotty analyses, K was not measured in the same sample as Ar, and we adopted a typical value of 0.13% for several analyses of whole rock samples given in the Compendium by Meyer 2008.) Note that the concentrations of ^{40}Ar in these samples are relatively high and variable, and no correlation exists between K and ^{40}Ar . For isochrons through the origin, these data would define apparent ages ranging from $\sim 0.5 \text{ Ga}$ to $\sim 6 \text{ Ga}$.

Figure 17 is a similar plot of K versus total Martian ^{40}Ar (trapped and in situ decay) for those analyses listed in Table 2 for which the shergottite formation age is around 170 Ma. (NWA 3171 melt, containing Martian atmosphere, is not plotted here, but is plotted in Fig. 16.) This includes results for Ar-Ar analyses of Y-793605 WR (Bogard and Garrison

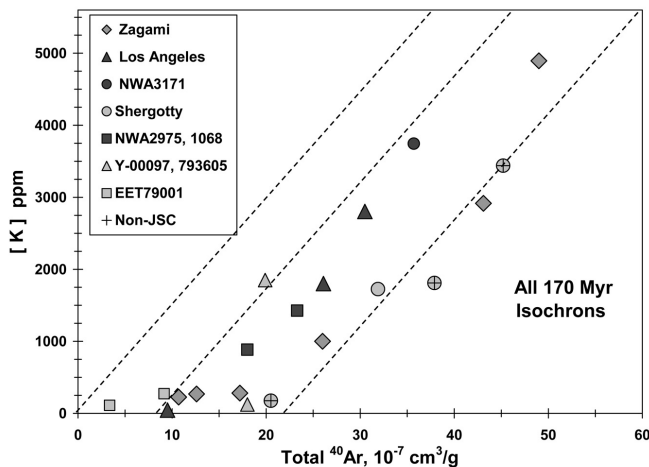


Fig. 17. Plot of total K versus total Martian ^{40}Ar for samples (WR, Plag, and Pyx) of shergottites possessing formation ages of approximately 170 Ma (Table 2). Shergotty points with a cross are from Terribilini et al. 1998. A minor terrestrial ^{40}Ar component has been subtracted. The dashed lines indicate hypothetical 170 Ma isochrons with different intercepts.

1999), Y-000097 Plag (Misawa et al. 2008), Zagami mineral separates (Bogard and Park 2008), and Shergotty whole rock and mineral separates where Ar and K were measured in the same sample (Bogard and Garrison 1999) and measured separately (Terribilini et al. 1998). We also plot results from Ar-Ar analyses of WR and Pyx of EET 79001, lithology A (Bogard and Garrison 1999). All of these shergottites have formation ages of ~ 170 – 190 Ma (Table 2).

Figure 17 illustrates two important characteristics also apparent from the preceding discussion. First, none of the data lie on a 170 Ma isochron passing through the origin. Rather, the higher the K content, the larger would be the apparent isochron age forced through the origin. If one fits a single isochron to all the JSC data, it gives an age of 215 ± 20 Ma and an ^{40}Ar intercept of $12 \times 10^{-7} \text{ cm}^3/\text{g}$. This emphasizes our earlier point that all of these samples contain trapped Martian ^{40}Ar above that expected from in situ decay. Secondly, if we pass 170 Ma isochrons through the data field, almost all samples are consistent with a 170 Ma age and a trapped ^{40}Ar component that varies only by a factor of about two, ~ 1 – $2 \times 10^{-6} \text{ cm}^3/\text{g}$. As discussed above, some of this variation in trapped ^{40}Ar may arise from measurement uncertainties and applied corrections. Note that samples plotted in Fig. 17 have a factor of 83 range in K content, which is several times greater than samples plotted in Fig. 16. However, samples in Fig. 17 have a range of ^{40}Ar concentrations only one-tenth as large as samples plotted in Fig. 16. For reasons given above, the trapped ^{40}Ar displayed in Fig. 17 is unlikely to be Martian atmosphere that was shock-implanted or adsorbed on weathered grain surfaces. Given the different degrees of shock heating of shergottites (Fritz et al. 2005) and different Ar diffusivities in Plag and Pyx (Bogard 2009), it also is very

unlikely that this trapped ^{40}Ar is a diffusion residue from shergottites that formed 4 Ga ago, as suggested by Bouvier et al. (2005, 2008). (Also see Bogard and Park 2008 for a more detailed discussion of this conclusion.)

The systematics of Fig. 17 strongly suggests that major minerals of all these shergottites contain similar concentrations of trapped Martian ^{40}Ar that was not directly acquired from the Martian atmosphere. The most reasonable source of this trapped ^{40}Ar is from the magma from which these meteorites crystallized. Bogard and Park (2008) report a detailed Ar-Ar study of mineral separates of two lithologies of Zagami (Table 2), which crystallized at different stages in magma evolution. They concluded that the similarity of trapped Martian ^{40}Ar in different Zagami minerals and phases implied its acquisition from the magma, into which it was introduced from the source rock or from assimilated crustal rock. They suggested that the $^{40}\text{Ar}_{\text{xs}}$ concentration in Zagami magma was kept constant during magma rise and crystallization because of decreasing pressure and Ar degassing. Similar trapped ^{40}Ar concentrations may imply similar magma histories for all the shergottites plotted in Fig. 17. Most of these meteorites are basaltic and enriched in trace elements (see Introduction), and all have ~ 170 Ma formation ages. Symes et al. (2008) suggested these basaltic shergottite all derived from a common magma reservoir. However, Y-000097 and Y-793605 have been classed as lherzolitic shergottites, possessing intermediate levels of trace element enrichment (see Introduction). Symes et al. (2008) suggest younger lherzolitic shergottites derived from a deeper source region than younger basalts, but may have co-mingled with basaltic shergottites during eruption. The EET 79001 shergottite contains two phases in contact, one basaltic (phase B) and one (phase A) having an olivine, pyroxene-phyric character (Goodrich 2002). The only datum that significantly deviates from the data band defined by Fig. 17 is a pyroxene separate from phase A of EET 79001. However, both K and ^{40}Ar in this sample were very low and have large uncertainties. To the extent that all shergottites plotted in Fig. 17 may have derived at about the same time from a common or connected magma reservoirs, this may explain the observation that they show similar concentrations of ^{40}Ar acquired from that magma.

Figure 18 plots K versus total Martian ^{40}Ar for analyses of five shergottites in Table 2, for which formation ages are substantially older than ~ 170 Ma and are ~ 327 – 575 Ma. Four of these shergottites are classified as olivine-phyric. The fifth, QUE 94201, is classified as basaltic, although strongly depleted in LREE. However, all five of these shergottites have similar initial Sr and Nd isotopic compositions, suggesting that they derived from similar depleted, but not necessarily the same source regions, possibly by fractional crystallization (Symes et al. 2008). The data in Fig. 18 show more scatter than those in Fig. 17 and suggest similar, but more varied amounts of trapped Martian ^{40}Ar of ~ 3 – $26 \times 10^{-7} \text{ cm}^3/\text{g}$. For

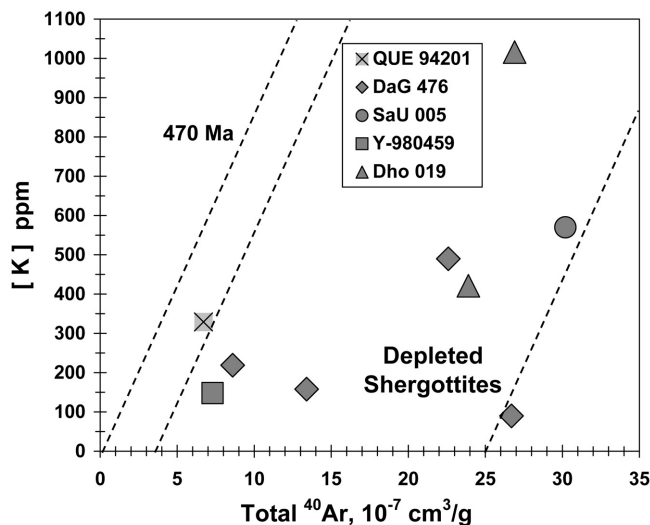


Fig. 18. Plot of total K versus total Martian ^{40}Ar for samples of olivine-phyric shergottites possessing formation ages between ~ 327 and ~ 575 Ma. All samples are WR, except that QUE is a Plag separate. A minor terrestrial ^{40}Ar component has been subtracted for each sample. The dashed lines indicate hypothetical 470 Ma isochrons with different intercepts.

DaG 476 and Dho 019, corrections for terrestrial ^{40}Ar made for the lower temperature extractions are large (Table 2) and may produce some of the scatter. However, less weathered SaU 005, Y-980459, and QUE 94201 also define extreme concentrations of trapped Martian ^{40}Ar . A case for excess Martian ^{40}Ar in these older shergottites having derived from the magma is weaker than for younger shergottites of Fig. 17, and some of this ^{40}Ar may be Martian atmosphere. Further, methods for acquiring this amount of ^{40}Ar from the magma of these depleted shergottites seem more restrictive than for the younger, enriched shergottites. For Zagami, Bogard and Park (2008) showed that the concentration of trapped ^{40}Ar , combined with Ar distribution coefficients between mafic minerals and magma, implied a relatively high ^{40}Ar concentration in the magma of $\sim 10^{-3} \text{ cm}^3/\text{g}$. Although this is consistent with Ar solubility in magma under the pressure thought to exist in the Zagami source region, it requires a relative high K concentration and a time of several Ga for this much ^{40}Ar to be produced by ^{40}K decay. Crustal or upper mantle rocks enriched in trace elements could possibly supply this much ^{40}Ar for basaltic shergottites, but this seems less likely for deep, depleted magma sources. Further, if these depleted magmas acquired their trapped ^{40}Ar by assimilation of crustal materials, this should be apparent in some other trace elements and isotopes. Thus, the origin of trapped Martian ^{40}Ar in depleted shergottites is unclear.

CONCLUSIONS

All ^{39}Ar - ^{40}Ar analyses of Martian shergottites give apparent ages that exceed their formation ages as defined by

Sm-Nd and Rb-Sr isochrons. When Ar-Ar data are examined in isochron plots, almost all samples still give isochron “ages” that are too old. Only Los Angeles Plag and possibly NWA 3171 Plag give Ar-Ar isochron ages in agreement with ages determined from other isotopic chronometers. All shergottites contain an excess Martian ^{40}Ar component not arising from in situ decay of K. Depending on the sample, this excess ^{40}Ar is located throughout the lattice, or concentrated in the K-bearing lattice, or both (Appendix 2). Although strongly shocked phases (e.g., impact melts) of some Martian shergottites contain implanted Martian atmospheric gases, trapped ^{40}Ar in many shergottites was not directly incorporated from the atmosphere. Similar concentrations of $^{40}\text{Ar}_{\text{xs}}$ ($\sim 1\text{--}2 \times 10^{-6} \text{ cm}^3/\text{g}$) occurs in mineral and WR samples of several younger shergottites, especially basaltic shergottites with formation ages of ~ 170 Ma, in spite of a variation in K concentration by a factor of ~ 80 . Similar $^{40}\text{Ar}_{\text{xs}}$ concentrations, association of at least part of this $^{40}\text{Ar}_{\text{xs}}$ with K, and the lack of a clear correlation between $^{40}\text{Ar}_{\text{xs}}$ and trapped ^{36}Ar suggest a common, non-atmospheric origin for this $^{40}\text{Ar}_{\text{xs}}$. In our previous and detailed Ar-Ar study of Zagami, we concluded that $^{40}\text{Ar}_{\text{xs}}$ was acquired from the magma. We suggest the same origin for $^{40}\text{Ar}_{\text{xs}}$ in other shergottites, especially younger (~ 170 Ma) basaltic and lherzolitic shergottites, which may share a common or linked magma sources (Symes et al. 2008). The original source of this $^{40}\text{Ar}_{\text{xs}}$ incorporated into the magma may represent assimilation of K-enriched crustal rock or degassing of source rock into the magma chamber(s).

Acknowledgments—We thank those individuals listed in Appendix 1 for supplying samples, and C-Y Shih and Y. Reese for preparing some of the mineral separates. We also thank L. Nyquist for permission to quote two of his unpublished shergottite ages. We thank T. Swindle, E. Walton, V. Fernandes, and an anonymous reviewer for valuable review comments. This research was supported by NASA’s Cosmochemistry Program. J. P. also acknowledges support of the NASA Postdoctoral Program.

Editorial Handling—Dr. Timothy Swindle

REFERENCES

- Barrat J. A., Jambon A., Bohn M., Gillet Ph., Sautter V., Göpel C., Lesourd M., and Keller F. 2002. Petrology and chemistry of the picritic shergottite North West Africa 1068 (NWA 1068). *Geochimica et Cosmochimica Acta* 66:3505–3518.
- Bartoschewitz R. and Ackermann D. 2001. Dar al Gani 876, a further fragment of the DaG-Shergottite (abstract). *Meteoritics & Planetary Science* 36:A15.
- Bartoschewitz R. and Appel P. 2003. Sayh al Uhaymir 150—A further fragment of the SaU-shergottite shower (abstract). *Meteoritics & Planetary Science* 38:A38.
- Bogard D. D. 2009. K-Ar dating of rocks on Mars: Requirements from Martian meteorite analyses and isochron modeling. *Meteoritics & Planetary Science* 44:3–14.

- Bogard D. D. and Garrison D. H. 1999. Argon-39–argon-40 “ages” and trapped argon in Martian shergottites, Chassigny, and Allan Hills 84001. *Meteoritics & Planetary Science* 34:451–473.
- Bogard D. D. and Park J. 2008. ^{39}Ar - ^{40}Ar dating of the Zagami Martian shergottite and implications for magma origin of excess ^{40}Ar . *Meteoritics & Planetary Science* 43:1113–1126.
- Bogard D. D., Garrison D. H., Norman M., Scott E. R. D., and Keil K. 1995. ^{39}Ar - ^{40}Ar age and petrology of Chico: Large-scale impact melting of the L chondrite parent body. *Geochimica et Cosmochimica Acta* 59:1383–1400.
- Bogard D. D., Garrison D. H., and McCoy T. J. 2000. Chronology and petrology of silicates from IIE iron meteorites: Evidence of a complex parent body evolution. *Geochimica et Cosmochimica Acta* 64:2133–2154.
- Borg L. E., Nyquist L. E., Taylor L. A., Wiesmann H., and Shih C.-Y. 1997. Constraints on Martian differentiation processes from Rb-Sr and Sm-Nd isotopic analyses of the basaltic shergottite QUE 94201. *Geochimica et Cosmochimica Acta* 61:4915–4931.
- Borg L. E., Nyquist L. E., Reese Y., Wiesmann H., Shih C.-Y., Ivanova M., Nazarov M. A., and Taylor L. A. 2001. The age of Dhofar 019 and its relationship to the other Martian meteorites (abstract #1144). 32th Lunar and Planetary Science Conference. CD-ROM.
- Borg L. E., Nyquist L. E., Wiesmann H., Shih C.-Y., and Reese Y. 2003. The age of Dar al Gani 476 and the differentiation history of the Martian meteorites inferred from their radiogenic isotopic systematics. *Geochimica et Cosmochimica Acta* 67:3519–3536.
- Borg L. E., Edmunson J. E., and Asmerom Y. 2005. Constraints on the U-Pb isotopic systematics of Mars inferred from a combined U-Pb, Rb-Sr, and Sm-Nd isotopic study of the Martian meteorite Zagami. *Geochimica et Cosmochimica Acta* 69:5819–5830.
- Bouvier A., Blichert-Toft J., Vervoort J. D., and Albarède F. 2005. The age of SNC meteorites and the antiquity of the Martian surface. *Earth & Planetary Science Letters* 240:221–233.
- Bouvier A., Blichert-Toft J., Vervoort J. D., Gillet P., and Albarède F. 2008. The case for old basaltic shergottites. *Earth & Planetary Science Letters* 266:105–124.
- Bunch T. E., Irving A. J., Wittke J. H., and Kuehner S. M. 2008. Highly evolved basaltic shergottite Northwest Africa 2800: A clone of Los Angeles (abstract #1953). 39th Lunar and Planetary Science Conference. CD-ROM.
- Christen F., Eugster O., and Busemann H. 2005. Mars ejection times and neutron capture effects of the nakhlites Y000593 and Y000749, the olivine-phyric shergottite Y980459, and the lherzolite NWA 1950. *Antarctic Meteorite Research* 18:117–132.
- Eugster O., Weigel A., and Polnau E. 1997. Ejection times of Martian meteorites. *Geochimica et Cosmochimica Acta* 61:2749–2759.
- Eugster O., Busemann H., Lorenzetti S., and Terribilini D. 2002. Ejection ages from krypton-81-krypton-83 dating and pre-atmospheric sizes of Martian meteorites. *Meteoritics & Planetary Science* 37:1345–1360.
- Folco L. and Franchi I. A. 2000. Dar al Gani 670 shergottite: A new fragment of the Dar al Gani 476/489 Martian meteorite (abstract). *Meteoritics & Planetary Science* 35:A54–55.
- Folco L., Franchi I. A., D’Orazio M., Rocchi S., and Schultz L. 2000. A new Martian meteorite from the Sahara: The shergottite Dar al Gani 489. *Meteoritics & Planetary Science* 35:827–839.
- Fritz J., Artemieva N., and Greshake A. 2005. Ejection of Martian meteorites. *Meteoritics & Planetary Science* 40:1393–1411.
- Garrison D. H. and Bogard D. D. 1998. Isotopic composition of trapped and cosmogenic noble gases in several Martian meteorites. *Meteoritics & Planetary Science* 33:721–736.
- Garrison D. H. and Bogard D. D. 2000. Cosmogenic and trapped Noble gases in the Los Angeles Martian meteorite (abstract). *Meteoritics & Planetary Science* 35:A58.
- Garrison D. H., Hamlin S., and Bogard D. D. 2000. Chlorine abundances in meteorites. *Meteoritics & Planetary Science* 35:419–429.
- Garrison D. H. and Bogard D. D. 2001. Argon-39-argon-40 “ages” and trapped argon for three Martian shergottites (abstract). *Meteoritics & Planetary Science* 36:A62–63.
- Gnos E., Hofmann B., Franchi I. A., Al-Kathiri A., Hauser M., and Moser L. 2002. Sayh al Uhaymir 094—A new Martian meteorite from the Oman desert. *Meteoritics & Planetary Science* 37:835–854.
- Goodrich C. A. 2002. Olivine-phyric Martian basalts: A new type of shergottite. *Meteoritics & Planetary Science* 37:B31–B34.
- Greshake A., Fritz J., and Stöffler D. 2003. Petrography and shock metamorphism of the unique shergottite Yamato 980459 (abstract). International Symposium. *Evolution of Solar System: A New Perspective from Antarctic Meteorites*, National Institute Polar Research, Tokyo:29–30.
- Greshake A., Fritz J., and Stöffler D. 2004. Petrology and shock metamorphism of the olivine-phyric shergottite Yamato 980459: Evidence for a two-stage cooling and single-stage ejection history. *Geochimica et Cosmochimica Acta* 68:2359–2377.
- Grossman J. N. 2000. The Meteoritical Bulletin, No. 84, August. *Meteoritics & Planetary Science* 35:A199–225.
- Grossman J. N. and Zipfel J. 2001. The Meteoritical Bulletin, No. 85, September. *Meteoritics & Planetary Science* 36:A293–A322.
- Herd C. D. K., Borg L. E., Jones J. H., and Papike J. J. 2002. Oxygen fugacity and geochemical variations in the Martian basalts: Implications for Martian basalt petrogenesis and the oxidation state of the upper mantle of Mars. *Geochimica et Cosmochimica Acta* 66:2025–2036.
- Hofmann B. A., Gnos E., Hauser M., Moser L., Al-Kathiri A., and Franchi I. A. 2001. The 2001 Omani-Swiss meteorite search campaign and recovery of shergottite Sayh al Uhaymir 094 (abstract). *Meteoritics & Planetary Science* 36:A82–83.
- Ikeda Y. 1997. Petrology and mineralogy of the Y-793605 Martian meteorite. *Antarctic Meteorite Research* 10:13–40.
- Ikeda Y. 2004. Petrology of the Yamato 980459 shergottite. *Antarctic Meteorite Research* 17:35–54.
- Irving A. J., Herd C. D. K., Kuehner S. M., Gregory D. A., and Aaronson A. A. 2005. Petrology and redox state of basaltic shergottite NWA 3171 (abstract). *Meteoritics & Planetary Science* 39:A49.
- Kojima H., Miyamoto M., and Warren P. H. 1997. The Yamato-793605 Martian meteorite consortium. *Antarctic Meteorite Research* 10:3–12.
- Marti K., Kim J. S., Thakur A. N., McCoy T. J., and Keil K. 1995. Signatures of the Martian atmosphere in glass of the Zagami meteorite. *Science* 267:1981–1984.
- Mathew K. J., Marty B., Marti K., and Zimmermann L. 2003. Volatiles (nitrogen, noble gases) in recently discovered SNC meteorites, extinct radioactivities and evolution. *Earth & Planetary Science Letters* 214:27–42.
- McCoy T. J., Taylor G. J., and Keil K. 1992. Zagami: Product of a two-stage magmatic history. *Geochimica et Cosmochimica Acta* 56:3571–3582.
- McCoy T. J., Wadhwa M., and Keil K. 1999. New lithologies in the Zagami meteorite: Evidence for fractional crystallization of a single magma unit on Mars. *Geochimica et Cosmochimica Acta* 63:1249–1262.
- McDougall I. and Harrison T. M. 1999. *Geochronology and thermochronology by the $^{40}\text{Ar}/^{39}\text{Ar}$ method*. Oxford University Press. 269 p.
- McSween H. Y. Jr. 1985. SNC meteorites: Clues to Martian petrologic evolution? *Reviews in Geophysics* 23:391–416.
- McSween H. Y. Jr., Grove T. L., Lentz R. C. F., Dann J. C., Holzheid

- A. H., Riciputi L. R., and Ryan J. G. 2001. Geochemical evidence for magmatic water within Mars from pyroxenes in the Shergotty meteorite. *Nature* 409:487–490.
- Meyer C. 2008. Mars Meteorite Compendium, <http://curator.jsc.nasa.gov/antmet/mmc/index.cfm>
- Mikouchi T. 2001. Mineralogical similarities and differences between the Los Angeles basaltic shergottites and the Asuka-881757 lunar mare meteorite. *Antarctic Meteorite Research* 14: 1–20.
- Mikouchi T. and Miyamoto M. 1997. Yamato-793605: A lherzolite shergottite from Japanese Antarctic meteorite collection. *Antarctic Meteorite Research* 10:41–60.
- Mikouchi T. and Miyamoto M. 2002a. Olivine cooling rate of the Northwest Africa 1068 shergottite (Abstract #1346). 33rd Lunar and Planetary Science Conference. CD-ROM.
- Mikouchi T. and Miyamoto M. 2002b. Mineralogy and olivine cooling rate of the Dhofar 019 shergottite. *Antarctic Meteorite Research* 15:122–142.
- Mikouchi T. and Kurihara T. 2007. Y000027, Y000047 and Y000097: Mineralogy and petrology of paired Yamato 00 lherzolitic shergottites (abstract). 31st Symposium on Antarctic Meteorites. pp. 52–53.
- Mikouchi T., Miyamoto M., and McKay G. A. 2001. Mineralogy and petrology of the Dar al Gani 476 Martian meteorite: Implications for its cooling history and relationship to other shergottites. *Meteoritics & Planetary Science* 36:531–548.
- Mikouchi T., Koizumi E., McKay G., Monkawa A., Ueda Y., Chokai J., and Miyamoto M. 2004. Yamato 980459: Mineralogy and petrology of a new shergottite-related rock from Antarctica. *Antarctic Meteorite Research* 17:13–34.
- Mikouchi T., Kurihara T., and Miyamoto M. 2008. Petrology and mineralogy of RBT 04262: Implications for stratigraphy of the lherzolitic shergottite igneous block. (abstract #2403). 39th Lunar and Planetary Science Conference. CD-ROM.
- Misawa K., Yamada K., Nakamura N., Morikawa N., Yamashita K., and Premo W. R. 2006a. Sm-Nd isotopic systematics of lherzolitic shergottite Yamato-793605. *Antarctic Meteorite Research* 19:45–57.
- Misawa K., Iwata N., Imae N., Franchi I. A., Greenwood R. C., and Kojima H., 2006b. New lherzolitic shergottites from the Yamato Mountains (abstract). 30th Symposium on Antarctic Meteorites. pp. 63–64.
- Misawa K., Park J., Shih C.-Y., Reese Y., Bogard D. D., and Nyquist L. E. 2008. Rb-Sr, Sm-Nd and Ar-Ar isotopic systematics of lherzolitic shergottite Yamato 000097. *Polar Science* 2:163–174.
- Nagao K., Nakamura T., Miura Y.N., and Takaoka N. 1997. Noble gas and mineralogy of primary igneous materials of Y-793605 shergottite. *Antarctic Meteorite Research* 10:125–142.
- Nagao K., Park J., and Choi H.-G. 2008. Noble gases of the Yamato 000027 and Yamato 000097 lherzolitic shergottites from Mars. *Polar Science* 2:195–214.
- Nyquist L. E., Bogard D. D., Shih C. -Y., Greshake A., Stöffler D., and Eugster O. 2001a. Ages and geologic histories of Martian meteorites. *Space Science Reviews* 96:105–164.
- Nyquist L. E., Reese Y., Wiesmann H., and Shih C.-Y. 2001b. Age of EET 79001B and implications for shergottite origins (abstract #1407). 32nd Lunar and Planetary Science Conference. CD-ROM.
- Nyquist L., Bogard D., Yamaguchi A., Shih C.-Y., Karouji Y., Ebihara M., Reese Y., Garrison D., McKay G., and Takeda H. 2006. Feldspathic clasts in Yamato-86032: Remnants of the lunar crust with implications for its formation and impact history. *Geochimica et Cosmochimica Acta* 70:5990–6015.
- Okazaki R. and Nagao K. 2004. Noble gases of Yamato 980459 shergottite. *Antarctic Meteorite Research* 17:68–83.
- Park J. 2005. Noble gas study of Martian meteorites: New insights on Mars. Ph.D. thesis, University of Tokyo, Japan.
- Park J., Okazaki R., and Nagao K. 2003. Noble gas studies of Martian meteorites: Dar al Gani 476/489, Sayh al Uhaymir 005/060, Dhofar 019, Los Angeles 001, and Zagami (abstract #1213). 34th Lunar and Planetary Science Conference. CD-ROM.
- Park J., Garrison D. H., and Bogard D. D. 2009. ³⁹Ar-⁴⁰Ar ages of Martian nakhlites. *Geochimica et Cosmochimica Acta* 73:2177–2189.
- Rubin A. E., Warren P. H., Greenwood J. P., Verish R. S., Leshin L. A., and Hervig R. L. 2000. Petrology of Los Angeles: A new basaltic shergottite find (abstract #1963). 31st Lunar and Planetary Science Conference. CD-ROM.
- Russell S. S., Zipfel J., Grossman J. N., and Grady M. M. 2002. The Meteoritical Bulletin, No. 86, July. *Meteoritics & Planetary Science* 37:A157–A184.
- Russell S. S., Zipfel J., Folco L., Jones R., Grady M. M., McCoy T., and Grossman J. N. 2003. The Meteoritical Bulletin, No. 87, July. *Meteoritics & Planetary Science* 38A:189–A248.
- Schwenzer S. P., Herrmann S., Mohapatra R. K., and Ott U. 2007. Noble gases in mineral separates from three shergottites: Shergotty, Zagami, and EETA79001. *Meteoritics & Planetary Science* 42:387–412.
- Shih C.-Y., Nyquist L. E., Wiesmann H., and Barrat J. A. 2003. Age and petrogenesis of picritic shergottite NWA 1068: Sm-Nd and Rb-Sr isotopic study. (abstract #1439). 34th Lunar and Planetary Science Conference. CD-ROM.
- Shih C.-Y., Nyquist L. E., Wiesmann H., Reese Y., and Misawa K. 2005. Rb-Sr and Sm-Nd dating of olivine-phyric shergottite Yamato 980459: Petrogenesis of depleted shergottites. *Antarctic Meteorite Research* 18:46–65.
- Shih C.-Y., Nyquist L. E., and Reese Y. 2007. Rb-Sr and Sm-Nd isotopic studies of Martian depleted Shergottites SaU 094/005 (abs#1745). 38th Lunar and Planetary Science Conference. CD-ROM.
- Shukolyukov Y. A., Nazarov M. A. and Schultz L. 2002. A new Martian meteorite: The Dhofar 019 shergottite with an exposure age of 20 million years. *Solar System Research* 36:125–135. *Translated from Astronomicheskii Vestnik* 36:140–150.
- Swindle T. D. 2002. Martian noble gases. In *Noble gases*, edited by Pocerli D., Ballentine C. J., and Wieler R. Reviews in Mineralogy and Geochemistry, vol. 47. Mineralogical Society of America. pp. 171–190.
- Symes S. J. K., Borg L. E., Shearer C. K., and Irving A. J. 2008. The age of the Martian meteorite Northwest Africa 1195 and the differentiation history of the shergottites. *Geochimica et Cosmochimica Acta* 72:1696–1710.
- Taylor L. A., Nazarov M. A., Shearer C. K., McSween, Jr. H. Y., Cahill J., Neal C. R., Ivanova M. A., Barsukova L. D., Lentz R. C., Clayton R. N., and Mayeda T. K. 2002. Martian meteorite Dhofar 019: A new shergottite? *Meteoritics & Planetary Science* 37: 1107–1128.
- Terrilini D., Eugster O., Burger M., Jakob A., and Krähenbühl U. 1998. Noble gases and chemical composition of Shergotty mineral fractions, Chassigny, and Yamato 793605: The trapped argon-40/argon-39 ratio and ejection times of Martian meteorites. *Meteoritics & Planetary Science* 33:677–684.
- Wadhwa M., Lentz R. C. F., McSween H. Y., and Crozaz G. 2001. A petrologic and trace element study of Dar al Gani 476 and Dar al Gani 489: Twin meteorites with affinities to basaltic and lherzolitic shergottites. *Meteoritics & Planetary Science* 36:195–208.
- Warren P. H. and Bridges J. C. 2005. Geochemical subclassification of shergottites and the crustal assimilation model (abstract #2098). 36th Lunar and Planetary Science Conference. CD-ROM.
- Walton E. L., Kelly S. P., and Spray J. G. 2007. Shock implantation of Martian atmospheric argon in four basaltic shergottites: A laser probe ⁴⁰Ar/³⁹Ar investigation. *Geochimica et Cosmochimica Acta* 71:497–520.

- Williamson J. H. 1968. Least-squares fitting of a straight line. *Canadian Journal Physics* 46:1845–1847.
- Wittke J. H., Bunch T. E., Irving A. J., Farmer M., and Strope J. 2006. Northwest Africa 2975: An evolved basaltic shergottite with vesicular glass pockets and trapped melt inclusions (abstract #1368). 37th Lunar and Planetary Science Conference. CD-ROM.
- Xirouchakis D. M., Draper D. S., Schwandt C. S., and Lanzirotti A. 2002. Crystallization conditions of Los Angeles, a basaltic Martian meteorite. *Geochimica et Cosmochimica Acta* 66:1867–1880.
- Zipfel J. 2000. Sayh al Uhaymir 005/008 and its relationship to Dar al Gani 476/489 (abstract). *Meteoritics & Planetary Science* 35: A178.
- Zipfel J., Scherer P., Spettel B., Dreibus G., and Schultz L. 2000. Petrology and chemistry of the new shergottite Dar al Gani 476. *Meteoritics & Planetary Science* 35:95–106.

APPENDIX 1. DESCRIPTIONS AND SOURCES OF ANALYZED METEORITES

Two samples of the Los Angeles basaltic shergottite were found in 1999 in southern California (Grossman 2000). The meteorite has a high content of plagioclase (maskelynite, 43–54 %) and pyroxene (38–42%) and closely resembles Zagami and Shergotty (Rubin et al. 2000; Mikouchi 2001; Xirouchakis et al. 2002). We obtained our Los Angeles sample from C. Moore of Arizona State University. The Northwest Africa (NWA) 3171 basaltic shergottite (506 g) has a relatively fresh appearance and shows a pattern of subcalcic augite core and pigeonite rims similar to Zagami, Shergotty, and NWA 1669 (A. Irving, per. comm., 2005). It contains veins of black impact glass, and is not paired with any other NWA basaltic shergottites. Our NWA 3171 sample was obtained courtesy of A. Gregory and A. Irving of Washington. Hundreds of small pieces of basaltic shergottite NWA 2975, with total weight of 1.6 kg, were recovered at a strewn field in Algeria (Wittke et al. 2006; Bunch et al. 2008). NWA 2975 has 57.3 vol% pyroxene, 38.3 vol% plagioclase (maskelynitized), other accessory minerals, and prominent black glass and melt inclusions (Meyer 2008). Our sample of NWA 2975 was provided by A. Irving.

Yamato Y-000097, a lherzolitic shergottite recovered in Antarctica in 2000, is paired with Y-000027 and Y-000047. These meteorites contain olivine, low-Ca pyroxene, and maskelynitized plagioclase (Misawa et al. 2006b), and have similar petrographic features with other lherzolitic shergottites (Mikouchi and Kurihara 2007). Our Y-000097 sample was obtained from Japan National Institute for Polar Research through K. Nagao. Lherzolitic shergottite Y-793605 has strong affinity with other lherzolitic shergottites, ALH 77005 and LEW 88516 (Mikouchi and Miyamoto 1997). It is composed of 35–40 vol% olivine, 50–60 vol% pyroxene and 5–8 vol% maskelynitized plagioclase (Kojima et al. 1997; Ikeda 1997; Mikouchi and Miyamoto 1997). Our sample of Y-793605 was obtained from the Japan National Institute for Polar Research.

NWA 1068 is an olivine phyric shergottite, discovered in Morocco in 2001, and shows no fusion crust. It is thought to be paired with NWA 1110 (Meyer 2008), and NWA 1183 and NWA 1775 may also be paired (Russell et al. 2003). NWA 1068 is composed of 21–27 vol% olivine, ~50 vol% pyroxene,

16–22 vol% maskelynitized plagioclase and other minor minerals (Barrat et al. 2002; Mikouchi and Miyamoto 2002a). Our sample of NWA 1068 was obtained from J. Barrat of Université de Bretagne Occidentale, France. Dhofar 019 is an olivine phyric shergottite discovered in the Oman desert in 2000 (Grossman 2000). It contains 61–65 vol% pyroxene, 20–26 vol% maskelynitized plagioclase, and 9–14 vol% olivine (Taylor et al. 2002; Mikouchi and Miyamoto 2002b). Alone among the shergottites, Dho 019 has a relatively long cosmic-ray exposure (CRE) age of 20 Ma (Shukolyukov et al. 2002; Park et al. 2003), indicating ejection from Mars in a separate event. Our sample of Dho 019 was obtained from M. Nazarov (Vernadsky Institute of Geochemistry, Moscow) and L. A. Taylor (University of Tennessee). DaG 476 is an olivine-orthopyroxene shergottite found in Libya in 1998 (Zipfel et al. 2000). DaG 489, DaG 670, DaG 735, DaG 876, DaG 975 were reported as paired with DaG 476 (Folco et al. 2000; Folco and Franchi 2000; Bartoschewitz and Ackermann 2001; Russell et al. 2003). DaG 476 has ~20 vol% olivine megacrysts (phenocrysts with 5mm maximum radius) within a fine-grained groundmass of ~60 vol% pyroxene, 12–17 vol% maskelynitized plagioclase, and other minor minerals (Zipfel et al. 2000; Mikouchi et al. 2001; Folco et al. 2000; Wadhwa et al. 2001). Our sample of DaG 476 was obtained from K. Nagao of the University of Tokyo.

Yamato Y-980459 is an olivine phyric shergottite discovered near Minami-Yamato Nunataks in 1998. It is composed of 9–26 vol% olivine (including olivine megacrysts), 48–63 vol% pyroxene, and 25–37% plagioclase/maskelynite and glassy mesostasis, and is very depleted in light rare-earth-elements (Greshake et al. 2003, 2004; Ikeda 2004; Mikouchi et al. 2004). Our sample of Y-980459 was obtained from the Japan National Institute for Polar Research. Sayh al Uhaymir (SaU) 005 is an olivine phyric shergottite recovered in Oman in 1999. It is paired with SaU 008, SaU 051, SaU 094, SaU 060, SaU 090, SaU 120, and SaU 150 (Zipfel 2000; Hofmann et al. 2001; Grossman and Zipfel 2001; Gnos et al. 2002; Russell et al. 2002, 2003). SaU shergottites are similar to DaG in mineralogy and chemistry (Zipfel 2000). SaU is composed of ~50 vol% pyroxene, ~20–30 vol% olivine, and ~10 vol% maskelynite (Zipfel 2000; Gnos et al. 2002; Bartoschewitz and Appel 2003). Our sample of SaU 005 was obtained from B. Hoffman of the Bern Natural History Museum.

APPENDIX 2. DISCUSSION OF NON-STANDARD ARGON ISOCHRON PLOTS

Isochron plots for Martian shergottites are particularly complex because of the possible and common presence of many argon components (e.g., Bogard and Garrison 1999; Swindle 2002; Walton et al. 2007; Bogard and Park 2008). This is shown by the equation below for the $^{40}\text{Ar}/^{39}\text{Ar}$ ratio, which is the measured parameter that determines the derived isochron age:

$$[^{40}\text{Ar}/^{39}\text{Ar}]_{\text{total}} = \frac{[(^{40}\text{Ar}^* + ^{40}\text{Ar}_{\text{xs}})_{\text{K-phases}} + (^{40}\text{Ar}_{\text{xs}})_{\text{lattice}} + (^{40}\text{Ar}^*)_{\text{undegassed}} + (^{40}\text{Ar}_{\text{xs}})_{\text{shock-implanted}} \pm (^{40}\text{Ar})_{\text{weathering}}]}{[(^{39}\text{Ar})_{\text{K-phases}} + (^{39}\text{Ar})_{\text{weathering}} \pm (^{39}\text{Ar})_{\text{recoil}}]}$$

Here, $^{40}\text{Ar}^*$ is the component that decayed in situ from ^{40}K , $^{40}\text{Ar}_{\text{xs}}$ is an excess Martian component likely trapped from the magma and present in essentially all mineral phases of shergottites reported here (see Bogard and Park 2008). Shock-implanted Martian atmospheric ^{40}Ar is generally located in specific phases such as impact melt and usually can be avoided in sampling or recognized from the Ar isotopic composition (Bogard and Park 2008). Incorporation of ^{40}Ar into grain surfaces during weathering, either on Mars or Earth, loss or gain of $^{40}\text{Ar}^*$ during weathering, and K- ^{40}Ar separation during weathering generally appear only in the first few temperature extractions. These effects usually are revealed by unusually high or low ages, different K/Ca ratios, and especially high and rapidly decreasing $^{36}\text{Ar}/^{37}\text{Ar}$ ratios.

In a typical isochron plot normalized to ^{36}Ar , both $^{40}\text{Ar}_{\text{xs}}$ and ^{36}Ar exist in the lattice in separate locations from ^{39}Ar and $^{40}\text{Ar}^*$ and these are released in various mixing ratios as a function of extraction temperature. In many Martian meteorite samples, however, ^{36}Ar is not a single component, but consists of both cosmogenic ^{36}Ar and trapped ^{36}Ar , of which the latter may have multiple sources (e.g., terrestrial atmosphere, Martian atmosphere, Martian interior). The presence of multiple ^{36}Ar components, not correlated in their degassing as a function of temperature, can produce scattering on an isochron plot. There are two methods by which cosmogenic and trapped ^{36}Ar components sometimes can be resolved using measured $^{36}\text{Ar}/^{37}\text{Ar}$ ratios (see Garrison et al. 2000; Park et al. 2009). Resolution of $^{36}\text{Ar}_{\text{cos}}$ and trapped Martian ^{36}Ar sometimes can be made by assuming that the minimum measured $^{36}\text{Ar}/^{37}\text{Ar}$ ratio represents only $^{36}\text{Ar}_{\text{cos}}$. This method often is valid if several high-temperature extractions give relatively constant $^{36}\text{Ar}/^{37}\text{Ar}$ ratios. Alternatively, total $^{36}\text{Ar}_{\text{cos}}$ concentrations for a given shergottite may have been measured in un-irradiated samples or may be estimated from other shergottite analyses, if their CRE ages are believed to be similar (Park et al. 2009). In our data evaluations, we compare $^{36}\text{Ar}_{\text{cos}}$ obtained in this way with expected concentrations. Because shergottites contain

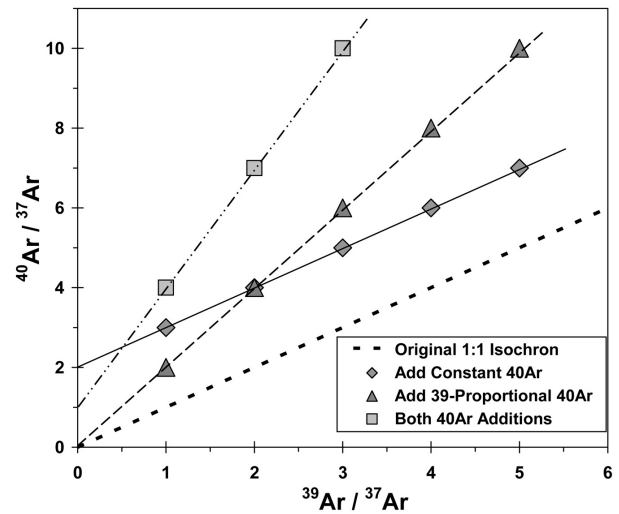


Fig. A1. Schematic effects of adding to a hypothetical isochron of slope 1 (dotted line) trapped ^{40}Ar located throughout lattice, trapped ^{40}Ar co-located with K and released in proportion to ^{39}Ar , and both types of trapped components.

substantial CI, which produces ^{38}Ar in the reactor, ^{38}Ar cannot be used in analyzing these Ar data.

We prefer to normalize these isochrons to ^{37}Ar , because total ^{36}Ar often cannot be reliably separated into distinct components. In contrast, ^{37}Ar is a single component produced in the reactor from Ca and is more abundant in the sample than is ^{36}Ar . Thus the $^{40}\text{Ar}/^{37}\text{Ar}$ and $^{39}\text{Ar}/^{37}\text{Ar}$ ratios are measured more precisely than ratios normalized to ^{36}Ar . The $^{39}\text{Ar}/^{37}\text{Ar}$ ratio is directly proportional to the K/Ca ratio. If an isochron plot normalized to ^{37}Ar yields a strongly linear correlation, then the slope ($^{40}\text{Ar}/^{39}\text{Ar}$ ratio) of that correlation is a measure of that ^{40}Ar in the sample which resides in the same lattice sites as K. The concentration of any $^{40}\text{Ar}_{\text{xs}}$ present throughout the sample lattice may be reflected in a positive intercept on the $^{40}\text{Ar}/^{36}\text{Ar}$ axis, just as with isochron plots normalized to ^{36}Ar . The $^{40}\text{Ar}/^{37}\text{Ar}$ intercept value will not represent a single Ar “component”. If the $^{39}\text{Ar}/^{37}\text{Ar}$ (K/Ca) ratios show little variation as a function of extraction temperature, then data will cluster on an isochron plot normalized to ^{37}Ar , and neither slope nor intercept values can be obtained.

An isochron plot where both $^{40}\text{Ar}^*$ and $^{40}\text{Ar}_{\text{xs}}$ are present can give varied results, depending on the mineral locations of the $^{40}\text{Ar}_{\text{xs}}$. This is demonstrated in Fig. A1. We start with a hypothetical isochron passing through the origin and having a slope of one. If we add $^{40}\text{Ar}_{\text{xs}}$ in constant amount to each temperature extraction, then the isochron shifts upward, maintains the same slope and age, and its $^{40}\text{Ar}/^{37}\text{Ar}$ intercept indicates the constant amount of $^{40}\text{Ar}_{\text{xs}}$ added. However, if we add an amount of $^{40}\text{Ar}_{\text{xs}}$ to each extraction that is not constant, but rather is proportional to the amount of ^{39}Ar in each extraction, then the isochron increases its slope (and apparent age), but still passes through the origin. Adding both $^{40}\text{Ar}_{\text{xs}}$

components in constant proportion increases the isochron slope still further and decreases its intercept, which still does not pass through the origin. Alternatively, if one component is preferentially added at low temperature and the other at high temperature, then a curved array of points might be produced, like that in Fig. 3. In shergottites, K is primarily located in feldspar (maskelynite) and possibly alkali-rich mesostasis (McDougall and Harrison 1999). Adding constant $^{40}\text{Ar}_{\text{xs}}$ to every extraction is equivalent to having $^{40}\text{Ar}_{\text{xs}}$ present throughout the lattice of all major minerals, including feldspar and pyroxene. In Fig. A1, this $^{40}\text{Ar}_{\text{xs}}$ would tend to occur in association with ^{37}Ar , the normalizing isotope produced from Ca, which by definition dominates the $^{40}\text{Ar}/^{37}\text{Ar}$ intercept at $^{39}\text{Ar}/^{37}\text{Ar} = 0$. Adding $^{40}\text{Ar}_{\text{xs}}$ in proportion to the amount of ^{39}Ar is equivalent to $^{40}\text{Ar}_{\text{xs}}$ occurring primarily in those lattice sites that contain significant K. Thus, an Ar-Ar isochron age older than the formation age indicates $^{40}\text{Ar}_{\text{xs}}$ located throughout the lattice; a positive isochron intercept indicates $^{40}\text{Ar}_{\text{xs}}$ located in K-bearing lattice sites; and both $^{40}\text{Ar}_{\text{xs}}$ components can be present.

In some cases, the Y-axis isochron intercept is negative, and these can be generated by counter-clockwise rotation of

the isochron. Such rotation could be produced by ^{39}Ar recoil loss from K-rich phases, which tend to plot far from the isochron origin (higher $^{39}\text{Ar}/^{37}\text{Ar}$), and ^{39}Ar recoil gain by Ca-rich phases, which tend to plot closer to the isochron origin (lower $^{39}\text{Ar}/^{37}\text{Ar}$). The presence of ^{39}Ar recoil redistribution during sample irradiation often can be inferred from the shape of the Ar-Ar age spectrum, and particularly from an age decrease for low K/Ca phases (e.g., pyroxene degassing at high temperatures) and an age increase for fine-grained K-rich phases, such as mesostasis or fine-grained feldspar (degassing at lower temperatures). In addition, isochron rotation and negative intercepts may be produced by excess ^{40}Ar incorporated into grain surfaces during weathering in either the Martian or terrestrial environment. Such $(^{40}\text{Ar})_{\text{weathering}}$ will tend to degas at lower extraction temperatures, and this can rotate counter-clockwise that part of the isochron giving higher $^{39}\text{Ar}/^{37}\text{Ar}$ ratios. Both ^{39}Ar recoil and ^{40}Ar incorporated into fine-grained phases or weathering products can increase isochron slope and apparent age, and both effects were observed and discussed for Martian nakhlites (Park et al. 2009).